AGU100 ADVANCING EARTH AND SPACE SCIENCE

Water Resources Research

RESEARCH ARTICLE
10.1029/2018WR023354

Special Section:
Big Data & Machine Learning in Water Sciences: Recent Progress and Their Use in Advancing Science

Downscaling SMAP Radiometer Soil Moisture Over the CONUS Using an Ensemble Learning Method

Peyman Abbaszadeh[1], **Hamid Moradkhani**[1], **and Xiwu Zhan**[2]

[1]Center for Complex Hydrosystems Research, Department of Civil, Construction and Environmental Engineering, University of Alabama, Tuscaloosa, AL, USA, [2]NOAA-NESDIS-STAR, College Park, MD, USA

Abstract Soil moisture plays a critical role in improving the weather and climate forecast and understanding terrestrial ecosystem processes. It is a key hydrologic variable in agricultural drought monitoring, flood forecasting, and irrigation management as well. Satellite retrievals can provide unprecedented soil moisture information at the global scale; however, the products are generally provided at coarse resolutions (25–50 km^2). This often hampers their use in regional or local studies. The National Aeronautics and Space Administration Soil Moisture Active Passive (SMAP) satellite mission was launched in January 2015 aiming to acquire soil moisture and freeze-thaw states over the globe with 2 to 3 days revisit frequency. This work presents a new framework based on an ensemble learning method while using atmospheric and geophysical information derived from remote-sensing and ground-based observations to downscale the level 3 daily composite version (L3_SM_P) of SMAP radiometer soil moisture over the Continental United States at 1-km spatial resolution. In the proposed method, a suite of remotely sensed and in situ data sets are used, including soil texture and topography data among other information. The downscaled product was validated against in situ soil moisture measurements collected from two high density validation sites and 300 sparse soil moisture networks throughout the Continental United States. On average, the unbiased Root Mean Square Error between the downscaled SMAP soil moisture data and in-situ soil moisture observations adequately met the SMAP soil moisture retrieval accuracy requirement of 0.04 m^3/m^3. In addition, other statistical measures, that is, Pearson correlation coefficient and bias, showed satisfactory results.

Key Points:
- Downscaled SMAP soil moisture at 1 km provides opportunities for fine resolution hydrologic modeling with operational implications
- The method uses a suite of atmospheric and geophysical information
- The downscaled SMAP is validated against measurements collected from core validation sites and 300 sparse soil moisture networks

Supporting Information:
- Supporting Information S1

Correspondence to:
P. Abbaszadeh,
pabbaszadeh@crimson.ua.edu

Citation:
Abbaszadeh, P., Moradkhani, H., & Zhan, X. (2019). Downscaling SMAP radiometer soil moisture over the CONUS using an ensemble learning method. *Water Resources Research*, *55*, 324–344. https://doi.org/10.1029/2018WR023354

Received 23 MAY 2018
Accepted 4 DEC 2018
Accepted article online 7 DEC 2018
Published online 14 JAN 2019

1. Introduction

Soil moisture has an important role in the global water and energy balance, affecting hydrological and atmospheric cycles, drought conditions, irrigation management, and so many other processes. Over the last decade, the development of remote sensing technologies has provided the possibility that this environmental variable is more accessible than before. Nowadays, remotely sensed satellite products have become the only feasible way to reach an unprecedented amount of soil moisture data on both spatial and temporal scales, which is practically unachievable from in situ observation networks (Kerr, 2007; Njoku & Entekhabi, 1996; Peng et al., 2016).

In the last couple of decades, although prodigious efforts have gone to retrieving soil moisture through various active and passive microwave remote sensing satellites, inevitably, they have some limitations. For example, active sensors like the European Remote-Sensing Satellite (ERS) provide observations that are significantly affected by the scattering produced by surface roughness (Verhoest et al., 2008) and vegetation structure (Wagner et al., 2013). Unlike the active sensors, passive microwave radiometers are much less sensitive to scattering, but their products are at coarse resolutions or their sensing depths are shallow (Molero et al., 2016). For instance, the Advanced Microwave Scanning Radiometer-Earth Observing System with C-band of 6.9 GHz has footprint of 74×43 km^2 that provides soil moisture from the 0–1- or 0–2-cm topsoil layer, while with smaller footprints, its X-band penetration depth is less than 5 mm (Su et al., 2013). In contrast, through L-band radiometer, the Soil Moisture and Ocean Salinity (SMOS) can estimate soil moisture at around 5-cm depth with a repeat cycle of ~3 days. This satellite has a coarse spatial resolution (35–55 km^2), which makes it inappropriate for local and regional scale applications (Djamai et al., 2016). Recent studies have shown that both the passive and active sensors have to come into play in order to access reliable remotely sensed soil moisture data (Owe et al., 2008; Petropoulos et al., 2015). Launched in 2015, the National Aeronautics and Space Administration (NASA) Soil Moisture Active Passive (SMAP) satellite provides high-resolution soil moisture on a global scale by combining L-band (passive) brightness temperatures and high

resolution L-band (active) radar backscatter data (Entekhabi, Njoku, et al., 2010). Unfortunately, due to a malfunction of the SMAP radar instrument on July 2015, since then the radiometer instrument has been the only operational instrument of SMAP satellite and been providing the level 2 soil moisture product (L2_SM_P; Chan et al., 2016). The assessment of SMAP radiometer observations corroborates the effectiveness of this procedure against Radio Frequency Interference (RFI) signals. Over densely vegetated areas where SMOS is more prone to RFI contamination, SMAP is more capable of retrieving soil moisture (Chan et al., 2016). Using brightness temperature, SMAP satellite provides soil moisture on the 36-km grid cell from both ascending (6:00 pm) and descending (6:00 am) passes.

Although the SMAP soil moisture observation has a decent spatial resolution for global and continental scale applications, it cannot be used directly for regional or local studies, such as agriculture and drought monitoring, unless a fine resolution of this product is available (from 1 to 10 km^2; Entekhabi, Njoku, et al., 2010). To circumvent this problem, on January 2017, NASA released a new product named the enhanced SMAP radiometer. In this data set, the standard SMAP data gridded at 36 km are interpolated into 9-km grid spacing using the Backus-Gilbert optimal interpolation algorithm. Despite such progress, some land surface applications such as water resources management, agricultural, and crop production still require soil moisture at finer resolutions, from a kilometer to subkilometer scale.

Over the last few years, a large number of approaches have been developed to downscale the coarse resolution of different satellite soil moisture products, such as SMOS (Djamai et al., 2015, 2016; Lievens et al., 2016; Merlin et al., 2008; Molero et al., 2016; Panciera et al., 2008; Piles et al., 2011, 2014, 2016) and Advanced Microwave Scanning Radiometer-Earth Observing System (Choi & Hur, 2012; Sahoo et al., 2013; Song et al., 2014; Zhao & Li, 2013). Among these attempts, Machine Learning (ML) techniques have recently received remarkable attention owing to their superb intelligence capability in downscaling satellite products (Alemohammad et al., 2018; Coulibaly et al., 2005; Goyal et al., 2012; Hashmi et al., 2011; Im et al., 2016; Kaheil et al., 2008; Kolassa et al., 2018; Raje & Mujumdar, 2011; Rodriguez-Fernandez et al., 2015; Srivastava et al., 2013; Valverde et al., 2014; Zerenner et al., 2016). ML is a class of data analysis methods that allows computers to find the hidden pattern of a phenomenon through learning from data in an intelligent way.

More investigations have shown that Random Forest (RF) algorithm in comparison with other ML approaches is more suitable for downscaling the satellite products (He et al., 2016; Hutengs & Vohland, 2016; Im et al., 2016; Jing et al., 2016; Ke et al., 2016; Park et al., 2017; Pelletier et al., 2016). This is due to the fact that RF model is much more flexible through randomization and adopts an ensemble approach. In this paper, we use the RF model in order to downscale the standard SMAP soil moisture radiometer product gridded at 36- to 1-km resolution over the Continental United States (CONUS) for the year 2015 (April to December). In this study, we develop multiple RF models based on soil properties of topsoil (0–5 cm) and use them collectively to better estimate the soil moisture not only at a finer spatial resolution but also over a very large region with different climate and land surface characteristics.

The rest of this paper is organized as follows. Section 2 summarizes both satellite and ground-based observations used in this research and describes concisely the study area. Section 3 elaborates on the developed soil moisture downscaling approach. The results and discussions are included in section 4. The conclusions of this paper and recommendations for future works are in the final section of the paper.

2. Remotely Sensed and Ground-Based Observations

2.1. SMAP Radiometer Soil Moisture Data

SMAP satellite with a sensing depth of 5 cm provides soil moisture on a global scale. Over the CONUS, SMAP was calibrated and validated against in situ measurements collected from several Core Validation Sites (CVSs) with the aim of reducing the unbiased Root Mean Square Error (ubRMSE) below 0.04 m^3/m^3 (Colliander, Jackson, et al., 2017; Jackson et al., 2016). In this study, we propose a soil moisture downscaling framework to downscale the SMAP descending overpass (L3_SM_P) over the CONUS. The L3_SM_P is a daily composite of L2_SM_P product. This soil moisture data can be assessed from the NASA Distributed Active Archive Center at the National Snow and Ice Data Center. We use the soil moisture product entitled "SMAP L3 Radiometer Global Daily 36 km EASE-Grid Soil Moisture, Version 3 (SPL3SMP)", which is available at https://nsidc.org/data/smap/smap-data.html.

2.2. MODIS Land Surface Temperature (LST) and Normalized Difference Vegetation Index (NDVI)

Over the past few years, vegetation index and surface temperature have been widely used for downscaling satellite soil moisture data (Fang & Lakshmi, 2014; Im et al., 2016; Merlin et al., 2008, 2015; Peng et al., 2015; Piles et al., 2011; Song et al., 2014; Srivastava et al., 2013). These land surface parameters are available from Moderate Resolution Imaging Spectroradiometer (MODIS) instrument. The common use of this geostationary satellite is due to its high temporal resolution that provides more cloud-free observations.

The MODIS is a key instrument of the NASA Earth Observing System Terra and Aqua platforms for monitoring the seasonality of global terrestrial vegetation. MODIS is a multispectral sensor. Its spectral bands range from visible, near infrared, to thermal infrared, making it ubiquitous in many land, ocean, and atmospheric research studies. The equatorial crossing time for Terra and Aqua satellites are 10:30 am (descending) and 1:30 pm (ascending), respectively. In this study, in order to be consistent with the SMAP data, the daytime overpass for Terra in the descending node is used to collect MODIS Land Surface Temperature (LST) and NDVI data. The MODIS products are the version-5 MODIS-Terra 1-km resolution daily LST data and the version-5 MODIS-Terra 1-km resolution 16-day NDVI data (data sets MOD11A1 and MOD13A2, respectively). MOD11A1 is composed of daytime and nighttime land surface temperatures. MOD13A2 is atmospherically corrected data set. The MODIS products are retrieved from the NASA Land Processes Distributed Active Archive Center at the United States Geological Survey (USGS) Earth Resources Observation and Science Center (http://e4ftl01.cr.usgs.gov/MOLT/).

2.3. NWS Precipitation Data

The most obvious way the atmosphere affects soil moisture is through precipitation (Crow et al., 2012). The soil moisture spatial and temporal variations are strongly correlated with the precipitation patterns. The teleconnection of precipitation regimes on the soil moisture variability has been corroborated by many studies at regional and global scales (Jones & Brunsell, 2009; Seneviratne et al., 2010). In this study, National Weather Service (NWS) precipitation data along with other atmospheric and geophysical information are used to investigate the usefulness of these climate variables in estimating soil moisture at finer resolution.

The NWS operations at the River Forecast Centers provide quality controlled and multisensor precipitation data with a spatial resolution of roughly 4 km^2 over the CONUS, Puerto Rico, and Alaska. The data are presented at 24-hourly accumulation that is the end of the "hydrologic day," a standard for river modeling. This product is primarily used to simulate streamflow across the CONUS (http://water.weather.gov/precip/).

2.4. CONUS-SOIL Data

Soil texture is defined as the proportion of small (clay), medium (silt), and large (sand) particles in a specific soil mass. This property of soil significantly affects the soil moisture profile, since it influences water infiltration rate, permeability, and water storage. Soil texture heterogeneity dominates the soil moisture spatial structure (Mattikalli et al., 1998). Many studies corroborated the utilization of soil texture data as an important source of information for downscaling soil moisture maps (Chakrabarti, Bongiovanni, et al., 2016; Mascaro et al., 2011; Ranney et al., 2015; Reichle et al., 2001; Shin & Mohanty, 2013).

In this study, we use soil texture information from the CONUS-SOIL data set. CONUS-SOIL data set is specifically used for regional climate and hydrologic modeling over the CONUS (Miller & White, 1998). This product is available at 1 km, which generates a spatial representation of soil texture and other properties of soil surface for a wide range of land surface models. CONUS-SOIL discretizes each soil property in 11 depth layers (up to 250 cm) where each layer is classified by 12 standard soil texture classes. Since SMAP provides soil moisture at the top 5 cm of the soil column, we only use the first layer of soil with depth of 5 cm to extract the soil texture information. Supporting information Figure S1 illustrates the soil texture of top 5-cm soil layer over the CONUS. CONUS-SOIL is available in both gridded and vector formats and can be retrieved via http://www.soilinfo.psu.edu/.

2.5. GTOPO30 Topography Data

Topographic data such as slope, aspect, curvature, and elevation significantly affect the distribution of soil moisture, specifically in the topsoil layer, at different scales (Crow et al., 2012). Elevation is known as one of the most effective topographic features in many studies to downscale coarse-scale soil moisture maps (Busch et al., 2012; Coleman & Niemann, 2013; Mascaro et al., 2011; Pellenq et al., 2003; Ranney et al., 2015;

Wilson et al., 2005). Hence, we use this variable in our proposed approach to downscale the SMAP soil moisture data.

GTOPO30 is a global Digital Elevation Model developed by USGS Earth Resources Observation and Science Data Center in late 1996. This data set has an approximately 1-km spatial resolution. Figure S2 shows the Digital Elevation Model with colors representing the variation of elevation from 0 to 4,587 m above sea level. More information along with the data set can be found at https://lta.cr.usgs.gov/GTOPO30. In this study, we used this data set, although there are other topography data products available, such as Shuttle Radar Topography Mission and National Elevation Dataset, which alternatively could be used.

2.6. In Situ Soil Moisture Observations

The U.S. Climate Reference Network (USCRN) sensors provide the soil information, such as soil moisture and soil temperature, at five different depths (5, 10, 20, 50, and 100 cm). Figure S2 demonstrates the USCRN stations located at 114 sites across the CONUS. The grid spacing of these sensors was determined so as to competently represent the U.S. annual temperature and precipitation variance. The soil moisture and soil temperature for each station are obtained from three independent samples of soil located in a 5-m radius around the main instrument tower. This leads not only to an accurate measurement of such quantities but also yields a more realistic representation of soil properties in a specified location. The USCRN records the soil moisture profile at 5-min intervals and transmits them as hourly data for satellite calibration/validation purposes.

The Soil Climate Analysis Network (SCAN) sensors monitor soil moisture content at five different depths (5, 10, 20, 50, and 100 cm approximately), air temperature, relative humidity, and some other climate variables mainly over the agricultural areas. In this study, we use 186 SCAN sensors that have been in operation for the period of the study. The SCAN sensors measure the soil moisture values hourly to aid different applications such as drought assessment/monitoring and satellite soil moisture validation. Both USCRN and SCAN sensors report the soil moisture in the volumetric unit (m^3/m^3). Figure S2 shows a map of SCAN soil moisture sensors located at 186 sites throughout the CONUS. USCRN instruments are scattered uniformly across the United States, while SCAN stations are installed in certain areas to accommodate specific research needs (Coopersmith et al., 2015). These two soil moisture networks have also been used for the validation of SMAP product (Jackson et al., 2016; Pan et al., 2016; Velpuri et al., 2015).

3. The Proposed Satellite Soil Moisture Downscaling Approach

This section elaborates the developed methodology in two separate subsections. In section 3.1, we present the theoretical basis of the proposed downscaling framework. Section 3.2 explains the ensemble learning algorithm used in section 3.1.

3.1. Soil Moisture Downscaling Framework

To downscale SMAP radiometer soil moisture, we use those high-resolution data sets that are known to be strongly associated with the soil moisture spatial and dynamical heterogeneities. As discussed in the previous section, the covariates including NDVI, surface temperature, precipitation, elevation, and soil texture are available at the appropriate resolutions and expected to have reasonable explanatory power on the soil moisture profile at different scales. Atmospheric covariates (i.e., precipitation and surface temperature) are used to maintain the temporal dynamics of the downscaled soil moisture. Geophysical covariates (i.e., soil texture and elevation) are included to capture the spatial patterns and variability of the downscaled soil moisture. Auxiliary covariates, such as NDVI (as a measure of greenness), are also included to account for the influence of vegetation dynamics on the downscaled soil moisture spatial and temporal patterns.

In this study, we use RF as an ensemble learning approach to formulate the downscaling framework. The basis of this technique and its implementation will be explained in detail later in section 3.2. The main contribution of this research is to introduce a new way to incorporate the aforementioned atmospheric and geophysical variables into the RF model, leading to improved estimates of soil moisture at finer resolutions. The following steps summarize the structure of the proposed soil moisture downscaling scheme.

1. Classify the in situ soil moisture stations (i.e., SCAN and USCRN) according to their soil texture properties. The results are shown in Table 1. As mentioned in section 2.4, only the soil texture of the top 5-cm soil

Table 1
Distribution of In Situ Soil Moisture Sensors Over CONUS With Respect to the Soil Texture of Top 5-cm Soil Layer

Soil texture	Soil texture acronym	Soil moisture stations		Total stations	% of CONUS
		USCRN	SCAN		
Bedrock	BR	—	—	—	0.001
Clay	C	3	6	9	3.384
Clay Loam	CL	4	8	12	4.210
Loam	L	28	41	69	24.552
Loamy Sand	LS	5	8	13	3.670
Other	O	1	0	1	1.545
Organic Materials	OM	2	0	2	1.176
Sand	S	13	11	42	6.977
Sandy Clay Loam	SCL	0	1	1	0.382
Silt	SI	0	0	0	0.004
Sandy Clay	SC	0	0	0	0
Silty Clay	SIC	1	1	2	1.506
Silty Clay Loam	SICL	7	14	21	4.395
Silty Loam	SIL	29	45	74	24.329
Sandy Loam	SL	21	51	72	22.603
Water	W	—	—	—	1.259
	Total	114	186	300	

Note. USCRN = U.S. Climate Reference Network; SCAN = Soil Climate Analysis Network; CONUS = Continental United States.

layer is used in this study in order to be consistent with the SMAP's sensing depth. Further investigation indicates that SCAN and USCRN in situ stations are distributed proportionally to be representative of different climate conditions and soil texture classes over CONUS. The study area is mostly dominated by loamy (24.5%), silty loam (24.3%), and sandy loam (22.6%) surface soil layers. These land surfaces encompass more than 200 stations for the soil moisture monitoring. Sandy clay loam, silty, and sandy clay soil types altogether cover less than 0.5% of the CONUS area. Only one station was found from the entire installed instruments throughout the CONUS that monitors the soil moisture for these rare land surfaces. As shown in Table 1, sandy loam with 22.6% surface soil coverage comprises 72 stations across CONUS, while clay loam with 4.2% encompasses 12 instruments. The same analogy can be applied to those regions characterized by sandy and loamy sand soil textures. This implies a relatively fair distribution of soil moisture instruments over the CONUS. It should be noted that some of the land surface layers are not considered in the proposed downscaling model since they either do not incorporate soil moisture stations (e.g., silty and sandy clay) or they include nonsoil layers (e.g., bedrock and water). Overall, these land surfaces cover a negligible (less than 0.5%) portion of the CONUS area.

As shown in Table 1, there are nine stations installed throughout the CONUS whose prevailing soil type is clay. It is important to know that these stations are not necessarily located on clay soil layer. Indeed, these stations are situated in the regions whose dominant soil type within a 1-km grid cell is clay.

2. Using those classified in-situ stations in the first step, we develop 12 distinct RF models. Each of these will downscale the SMAP radiometer soil moisture over a specific land surface layer. For example, for the clay soil type, nine stations provide a data collection with 2,448 rows and 6 columns. The 2,448 is calculated by 9×272, where 272 refers to the period of study (1 April 2015 until 31 December 2015). Six columns indicate five input covariates (including NDVI, surface temperature, precipitation, elevation, and SMAP soil moisture data) and one output variable (in situ soil moisture data). The dimension of this data set may decrease if it contains missing values. It is important to note that the input data are extracted from those points (latitudes and longitudes) where the in situ stations are located. In this study, we randomly separate 80% of the data collection to train the model, and the rest of the data (20%) is used to verify the model. By trial and error, we found that this set of model calibration and verification data set (80/20), although not significant, results in better model performance as compared to other combinations. The random splitting of the data set ensures that the developed model is able to generalize well to unseen data and to avoid overtraining. Thus, the developed RF model can be well suited for the soil moisture prediction at different geographical locations with different land-atmosphere characteristics.
3. The CONUS area is divided into different subregions based on the soil texture of the top 5-cm soil layer. The results in percentage of CONUS was reported in Table 1. The SMAP soil moisture over each of these regions is downscaled to 1-km spatial resolution using the corresponding calibrated RF model in step 2.

3.2. RF

The principle of the proposed downscaling approach is to build a function that maps the input covariates to the output variable using the following equations:

$$SM_d = f(C) + \varepsilon, \tag{1}$$

$$C = (c_1, c_2, c_3, \ldots c_N) \in \mathbb{R}^N, \tag{2}$$

where SM_d is the downscaled soil moisture data (response), C is an input vector, c_i represents the input covariates (i.e., precipitation, surface temperature, elevation, original SMAP, and NDVI), and N is the input

vector dimension (in this study N is equal to 5). In this formulation, depending on the relationship between response variables and input covariates, f can be a nonlinear or a linear function.

Although implementation of such regression-based model is easy, one drawback of this model is that it generally provides a single estimate and does not represent the uncertainty associated with the estimates. The approach taken in this study to characterize the uncertainty in our downscaling is the ensemble learning approach, such as RF. The idea of searching over random subset of decision rules while splitting nodes was first initiated by Amit and Geman (1997); later on, Breiman (2001) developed this idea and introduced the RF. RF is a ML technique, which is most appropriate for regression and classification problems. The adaptive, randomized, and decorrelated features of decision rules involved in RF make it more suitable approach when the relationship between the predictors and the response variable is complex and highly nonlinear. For a regression problem, first, a number of decision trees are built during the training phase, and then the mean prediction of these trees is calculated as the output of this approach. RF divides the input feature space into many regression trees, known as forest, where each tree is generated using a bootstrap sample. A bootstrap sample contains about two thirds of the training input data, and the left samples (one third) are used for the validation of each tree. This is one of the key features of RF algorithm (also known as out-of-bag samples) to estimate the model generalization error. This approach is based on the bagging (bootstrap aggregation) method that combines the results of many decision trees to reduce the chance of overfitting and improve the generalization. RF can be easily implemented in a parallel computing platform, which makes it more advantageous for large-scale problems (Breiman, 2001).

As previously mentioned, we randomly split the data set into two groups (using the 80% of data) to train and (using the 20% of data) to verify the RF model. The random splitting of the data set for model calibration and verification ensures the generalizability of the developed downscaling approach. In step 1, a bootstrap method is used to sample M subsets from the training data sets. In step 2, M independent regression trees are built to train the model using the bootstrapped samples. In step 3, the predicted value is obtained over M replications. In step 4, the final result is taken as the average of the individual tree outputs. This model selects a random subset of predictors in each decision tree to inject randomness in the RF model, which in turn alleviates the redundancy of predictors and diversifies the forecast decision trees (He et al., 2016).

The ensemble posterior is calculated by averaging M posteriors as follows: $p_t(SM_d|\, C)$ specifies the conditional distribution of the downscaled soil moisture (SM_d) given the bootstrapped samples from the training input covariate vector (C).

$$p(SM_d|C) = \frac{1}{M}\sum_{t=1}^{M} p_t(SM_d|C). \tag{3}$$

In this study, we used MATLAB TreeBagger built-in function to implement the RF algorithm. In the developed downscaling framework, each of the 12 RF models has been set to have 100 decision trees. This value was obtained using trial and error method, such that any value more than this does not improve the downscaling accuracy. This issue will be further discussed in the next section. Up to this point, we developed multiple RF models to map input covariates to a target variable. The next step is to implement the calibrated models on the test data sets to evaluate the model robustness and generalizability. Figure 1 depicts a schematic of the proposed soil moisture downscaling framework.

4. Results and Discussions

In this study, we discuss the results in three parts. Section 4.1 reports the performance of the developed RF models. Section 4.2 presents the comparison of the downscaled SMAP soil moisture products versus 300 sparse soil moisture networks throughout the CONUS. In section 4.3, the downscaled SMAP soil moisture data are validated against in situ soil moisture measurements collected from two CVSs.

4.1. Performance of the Proposed Downscaling Algorithm

In this study, we used the Pearson correlation coefficient "R" (Gan et al., 2014), "ubRMSE" (Entekhabi, Reichle, et al., 2010), and bias to measure the performance of the proposed downscaling algorithm. R is a common index to measure the strength of a linear association between two quantitative variables. The Pearson correlation coefficient is calculated at a 95% confidence level and ranges between -1 and 1. The bias measures

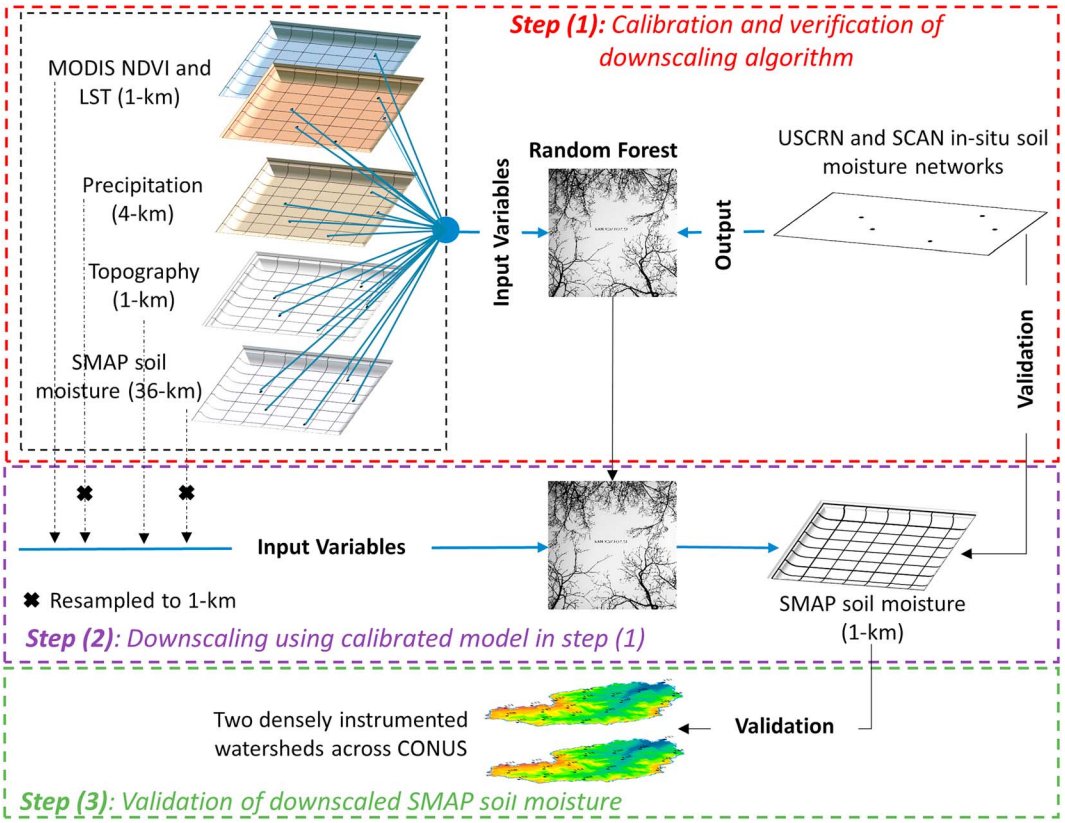

Figure 1. Schematic of the proposed soil moisture downscaling framework. MODIS = Moderate Resolution Imaging Spectroradiometer; SMAP = Soil Moisture Active Passive; USCRN = U.S. Climate Reference Network; SCAN = Soil Climate Analysis Network; CONUS = Continental United States.

the average tendency of overestimation (positive value) or underestimation (negative value) of the simulated data. The ideal value of bias is 0, showing a more accurate model simulation. The standard "RMSE" is very sensitive to biases in either the mean or the amplitude of variations. This bias can easily be removed by using the ubRMSE. The ubRMSE is a metric that SMAP uses to report the product accuracy. For soil moisture retrievals, the aforementioned metrics provide a more comprehensive description of product quality compared to other measures (Jackson et al., 2012). The SMAP mission requirement for soil moisture product accuracy is ubRMSE = 0.040 m^3/m^3 (Chan et al., 2016).

As mentioned earlier, the first step in developing the proposed downscaling scheme in this study is to calibrate and verify the RF models using the atmospheric and geophysical data sampled from locations where in situ observations are available. The distribution pattern of in situ soil moisture sensors over CONUS according to their soil texture properties makes it possible to develop 12 RF models to downscale soil moisture over more than 98% of the CONUS area. Figure 2 illustrates the performance of the developed soil moisture downscaling algorithm. Here we reported only the results of the verification step, which implies the ability of the calibrated models to generalize to unseen data. The statistical performance measures shown in this figure indicate that there is a very good agreement between the simulated and observed soil moisture values over different soil texture classes with different land-atmosphere couplings. In this study, we noticed that using only a single RF model would have generated a significant bias in model prediction and led to a worse model fit; however, as results indicate, multiple RF models classified based on the stations' soil texture properties simultaneously minimize the bias throughout the simulation process and enhance the model performance. The developed models based on those regions with abundant soil moisture stations (i.e., loamy, silty loam, and sandy loam) would be more reliable to predict the soil moisture and less prone to uncertainty than those areas with limited soil moisture sensors (i.e., silty clay and sandy clay loam). We also realized that although increasing the number of decision trees from 10 to 100 in random forest algorithm does not show

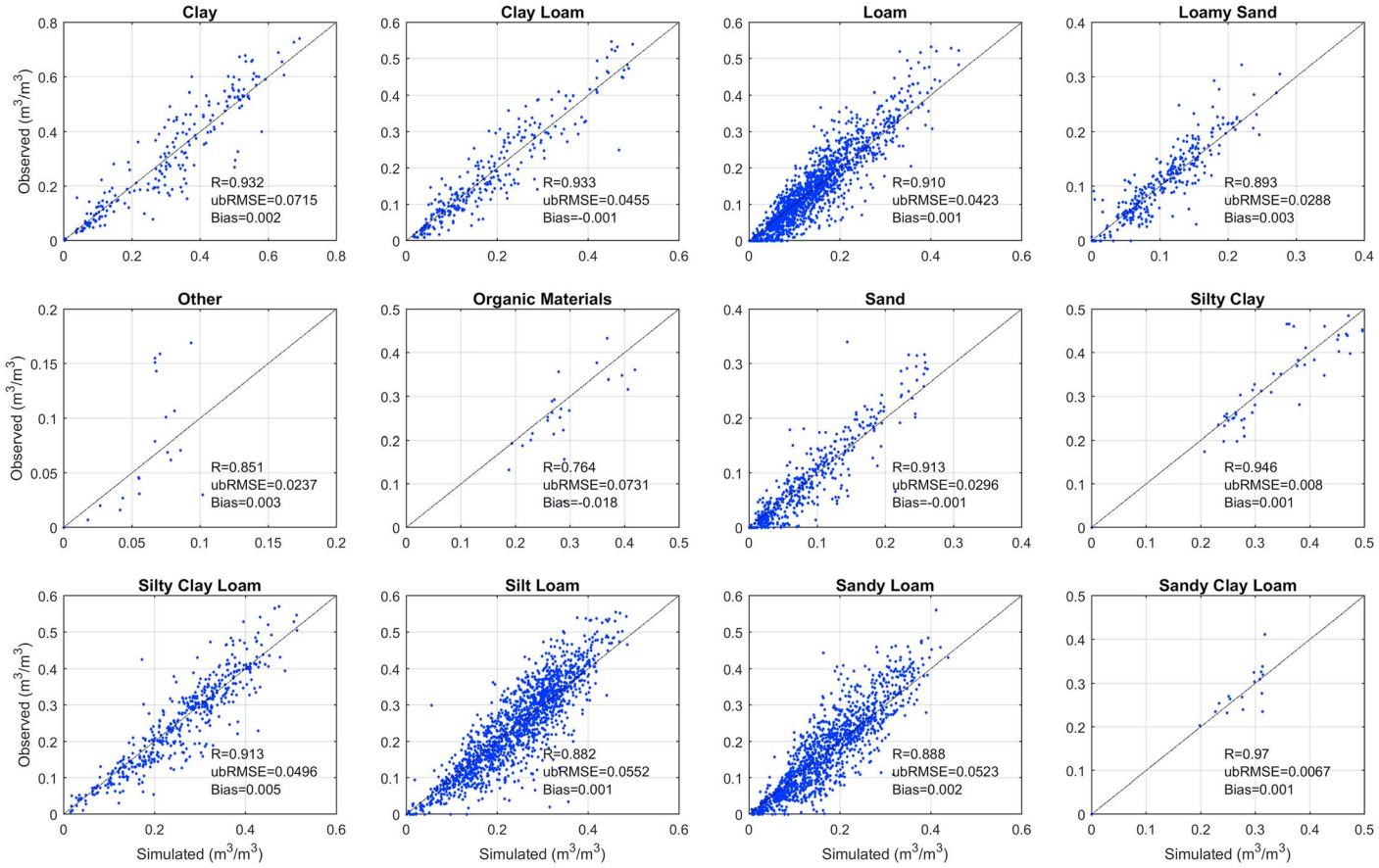

Figure 2. Verification results of the developed Random Forest models for each group of soil texture over Continental United States. ubRMSE = unbiased Root Mean Square Error.

significant improvement in model calibration and validation steps, it does so in downscaling step and generating the downscaled soil moisture data with higher accuracy. Also, it should be mentioned that using more than 100 decision trees does not enhance the downscaling accuracy and instead only makes the proposed approach computationally more intensive.

In the next step, these calibrated and verified models will be used to downscale the SMAP radiometer soil moisture from 36- to 1-km spatial resolution over CONUS for the period of 1 April 2015 to 31 December 2015.

4.2. Downscaled SMAP Soil Moistures Versus In Situ Observations

In this section, we compare the downscaled SMAP soil moistures at 1-km spatial resolution with those SCAN and USCRN in situ soil moisture observations scattered throughout the CONUS. Figure 3 reports the results indicating a consistently high correlation between the downscaled SMAP and in situ soil moistures almost everywhere across the CONUS except for a few isolated points with slightly low correlation in the Rocky Mountains. The same analogy and pattern is discernible for ubRMSE. The CONUS average correlation and ubRMSE values are highlighted in each subplot in Figure 3. The average correlations between downscaled SMAP and in situ data are 0.65 (SCAN) and 0.70 (CRN). The average ubRMSE is reported as 0.047 and 0.040 m^3/m^3, respectively, for SCAN and USCRN networks. More investigation also reveals a negligible amount of bias between the downscaled SMAP product and in situ observations. Such that the average bias is reported at 0.004 and 0.002 m^3/m^3, respectively, for SCAN and USCRN networks (not illustrated in Figure 3). These results are encouraging compared with those obtained from original SMAP soil moisture products as they show overestimation over arid regions with bare soils and underestimation over cold vegetated areas (Ma et al., 2017).

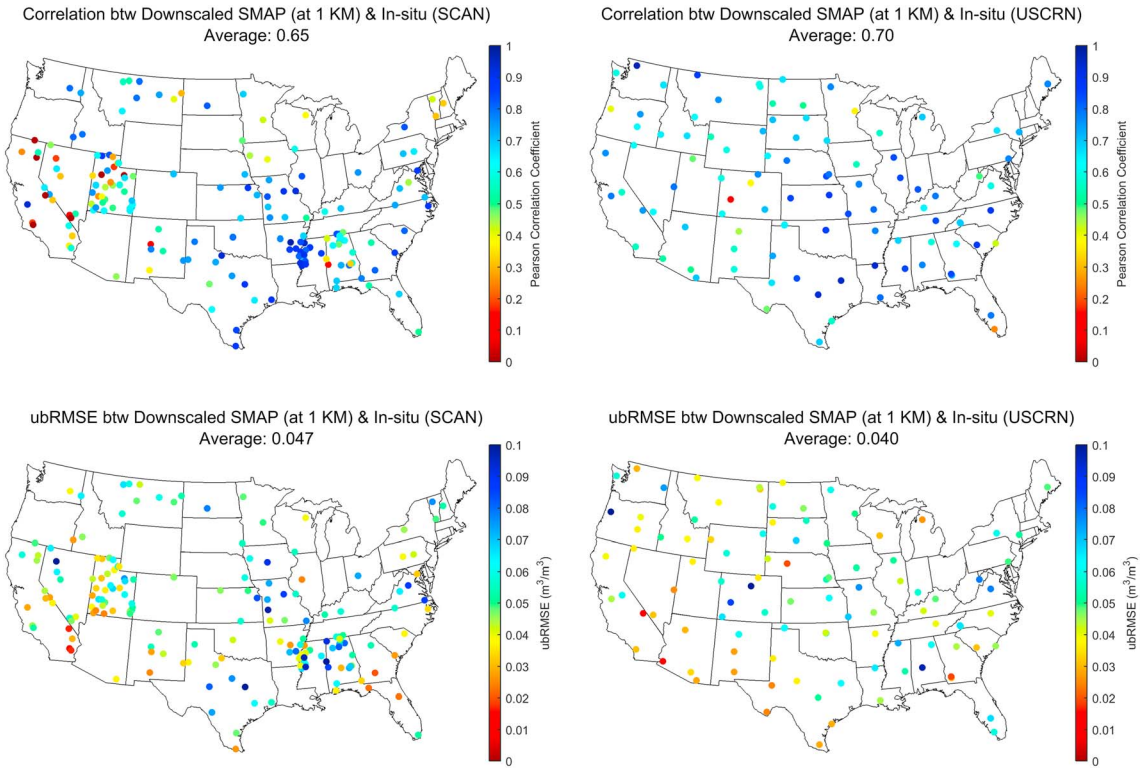

Figure 3. Correlation and ubRMSE calculated between in situ observations (SCAN and USCRN) and downscaled SMAP. ubRMSE = unbiased Root Mean Square Error; SCAN = Soil Climate Analysis Network; USCRN = U.S. Climate Reference Network; SMAP = Soil Moisture Active Passive.

For a few instruments on the East and West coasts, the model failed to meet the SMAP accuracy requirement (8 stations out of 300, not shown in Figure 3). The reason behind this may be attributed either to RFI signals that would contaminate the soil moisture retrievals over the stations located in densely vegetated areas or to the spatial mismatch of the SMAP footprint. Each of these cases may create an obstacle to retrieving the SMAP soil moisture data. For example, "CA Bodega 6 WSW" is one of those eight stations, which is located on the Pacific West Coast at Bodega Bay, California. This station is occupied by sandy soil. The SMAP pixel over this region may have been more susceptible either to the attenuation of microwave signal by the vegetation or to flooding due to heavy rainfall throughout the year. Hence, the SMAP pixel for this region is most often missing or discarded by the SMAP data quality flag, which leads to a worse downscaling result over corresponding in situ stations. Despite such limitation, the downscaled SMAP soil moistures correlate well with in situ observation networks over almost entire CONUS, including those mountainous and forested areas in the Eastern and Southeastern United States. These areas are generally challenging for retrieving soil moisture due to the attenuation of microwave signal by the vegetation. Figure 3 also implies the better performance of downscaled SMAP soil moisture over bare soils in comparison with vegetated soils.

Although the reported results are promising, they may not be fully indicative of the effectiveness of the proposed downscaling algorithm; therefore, we compare the results from the proposed approach with those obtained from a uniform disaggregation approach, where the value of fine-resolution grid cell is set to be the same value as its correspondent coarse-resolution grid cell. Figure 4 illustrates this comparison and shows that the proposed downscaling approach significantly outperforms the uniform disaggregation approach.

To analyze the importance of each input variable, that is, NDVI, surface temperature, precipitation, and topography, on the downscaling accuracy, we performed a leave-one-out approach where one input variable was removed and the downscaling was implemented. Therefore, the proposed downscaling algorithm is run under four different input schemes as follows:

Scheme 1. {NDVI, surface temperature, precipitation} + SMAP.
Scheme 2. {NDVI, surface temperature, topography} + SMAP.

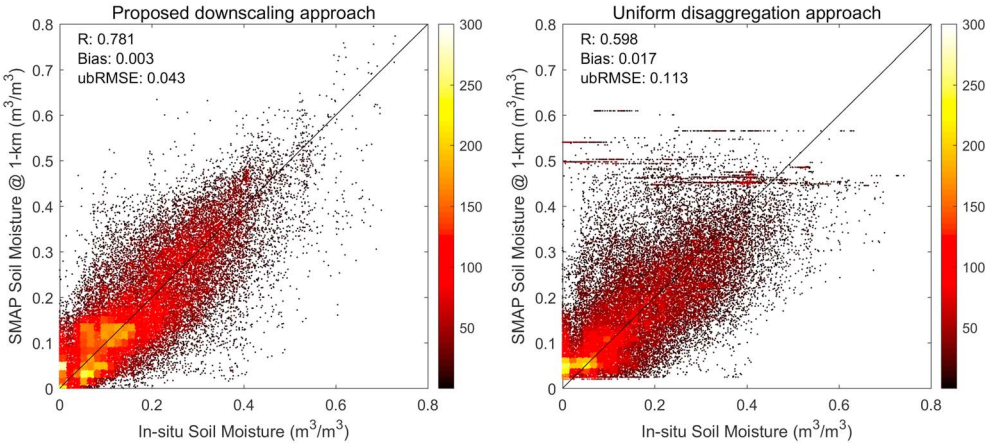

Figure 4. Comparison of downscaling accuracy between the proposed approach and the uniform disaggregation approach. Both Soil Climate Analysis Network and U.S. Climate Reference Network in situ observations were used in this analysis. ubRMSE = unbiased Root Mean Square Error; SMAP = Soil Moisture Active Passive.

Scheme 3. {surface temperature, precipitation, topography} + SMAP.
Scheme 4. {NDVI, precipitation, topography} + SMAP.

Figure 5 reports the results in four subplots. All three performance measures are also shown in this figure. The results confirmed that NDVI, surface temperature, and precipitation have almost similar influence on the downscaling accuracy; however, topography shows to be less influential than other variables on the results. By comparing the results in Figure 4 (where all input variables were taken into account) with those in this figure, it is seen that the inclusion of all input variables in the downscaling framework is essential for achieving the best downscaling accuracy. It is important to note that since the objective of this study is to downscale SMAP product, SMAP data must be included in all four input schemes.

In Figure 6, we use the Taylor (2001) diagram to provide a conclusive comparison between the performance of the downscaled SMAP by the proposed approach and the in situ soil moisture measurements at daily time scale collected from 186 SCAN and 114 USCRN stations scattered across the CONUS. The Taylor diagram graphically summarizes several important statistical indices to compare the similarity/dissimilarity between two patterns. This figure can be generated using three statistical metrics. Root Mean Square Difference (RMSD) is extensively used to assess the performance of satellite soil moisture products versus in situ measurements (Merlin et al., 2015). This metric integrates the three main components, namely, time series correlation, mean bias, and bias in the variance to evaluate the quality of data. The standard deviation ratio between the downscaled and in situ soil moisture is on the radial distance, and their correlation is on the angle of the polar plot. The black point shown in Figure 6 is named as the reference point, where all the metrics are considered optimal. The distance to this point indicates the centered normalized RMSD between the downscaled soil moisture and in situ soil moisture patterns.

The Taylor diagrams are showing most of the correlations above 0.7 for both SCAN and USCRN networks. It is also evident that most of the standard deviation ratios are less than 1 (black-dashed line in Figure 6), indicating the higher variability of in situ data compared to the downscaled data across almost all the stations in CONUS. It is, however, noted that a few stations end up inflating the standard deviation ratio. Further investigation revealed that the SMAP satellite has had poor performance over those sites due to the severe spatial heterogeneity (e.g., climate, topography, soil texture, vegetation, and land cover) that dominates the corresponding satellite's footprint.

4.2.1. Downscaled Soil Moisture Temporal Dynamic

The most reliable soil moisture downscaling technique should be able to satisfy two important criteria: first, the downscaled soil moisture estimates must capture the temporal dynamics of in situ soil moisture observations (Mishra et al., 2017; Peng et al., 2015; Piles et al., 2014), and second, the spatial pattern of the downscaled soil moisture data must follow that of the original soil moisture map (Kaheil et al., 2008; Kim & Barros, 2002; Piles et al., 2011; Sanchez et al., 2012). To investigate whether the downscaled soil moisture product would meet the temporal variability criterion, in this section, we evaluate the performance of the

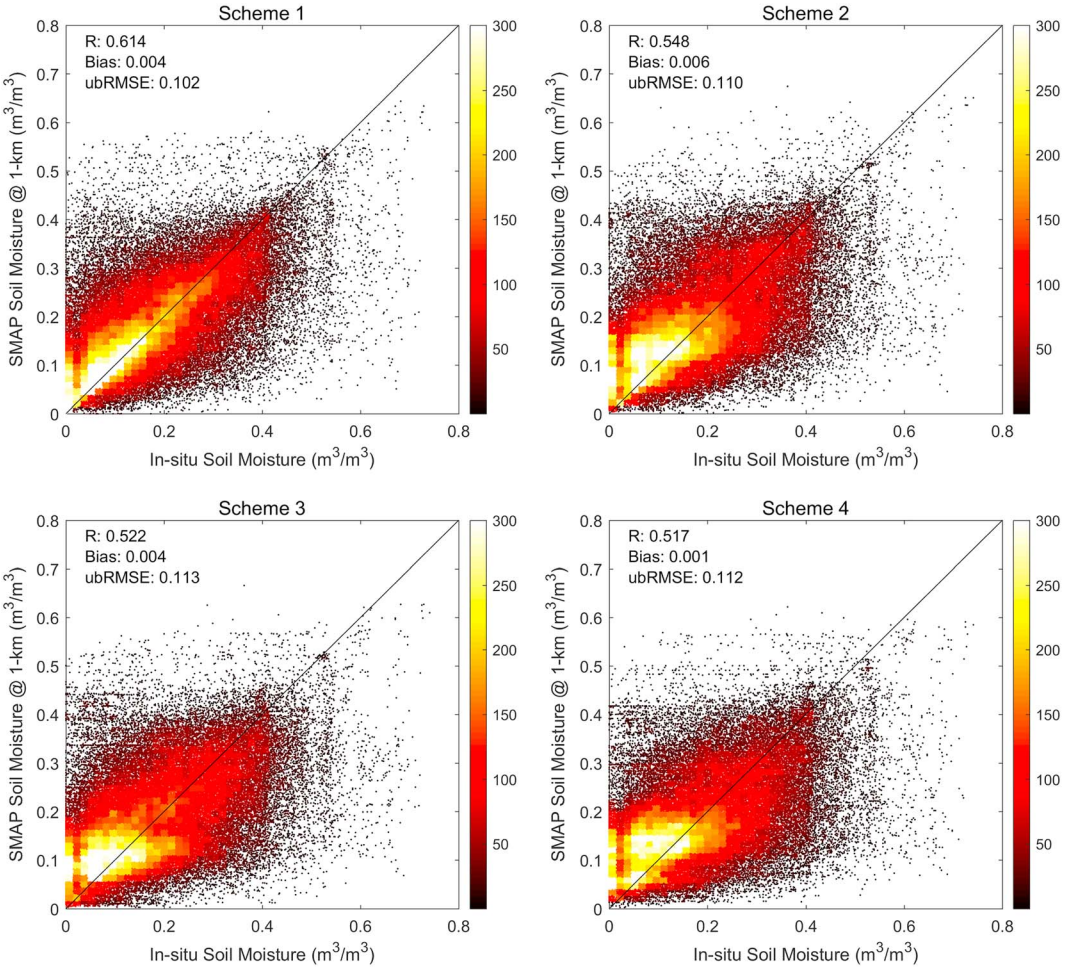

Figure 5. The performance of the proposed downscaling approach under four different input schemes. Both Soil Climate Analysis Network and U.S. Climate Reference Network in situ observations were used in this analysis. ubRMSE = unbiased Root Mean Square Error; SMAP = Soil Moisture Active Passive.

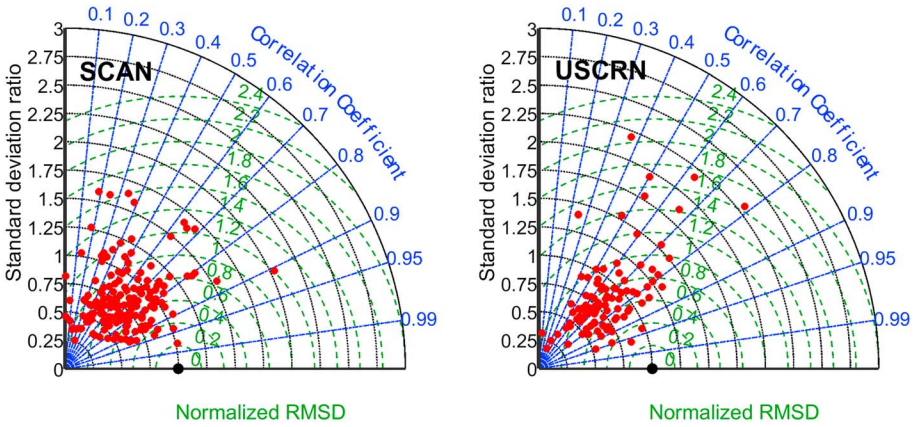

Figure 6. The accuracy of downscaled Soil Moisture Active Passive soil moisture versus in situ soil moisture observations collected from 186 SCAN and 114 USCRN stations for study period 01 April 2015 to 31 December 2015. RMSD is represented by green dashed line, while correlation coefficient is displayed by blue dotted line. SCAN = Soil Climate Analysis Network; USCRN = U.S. Climate Reference Network.

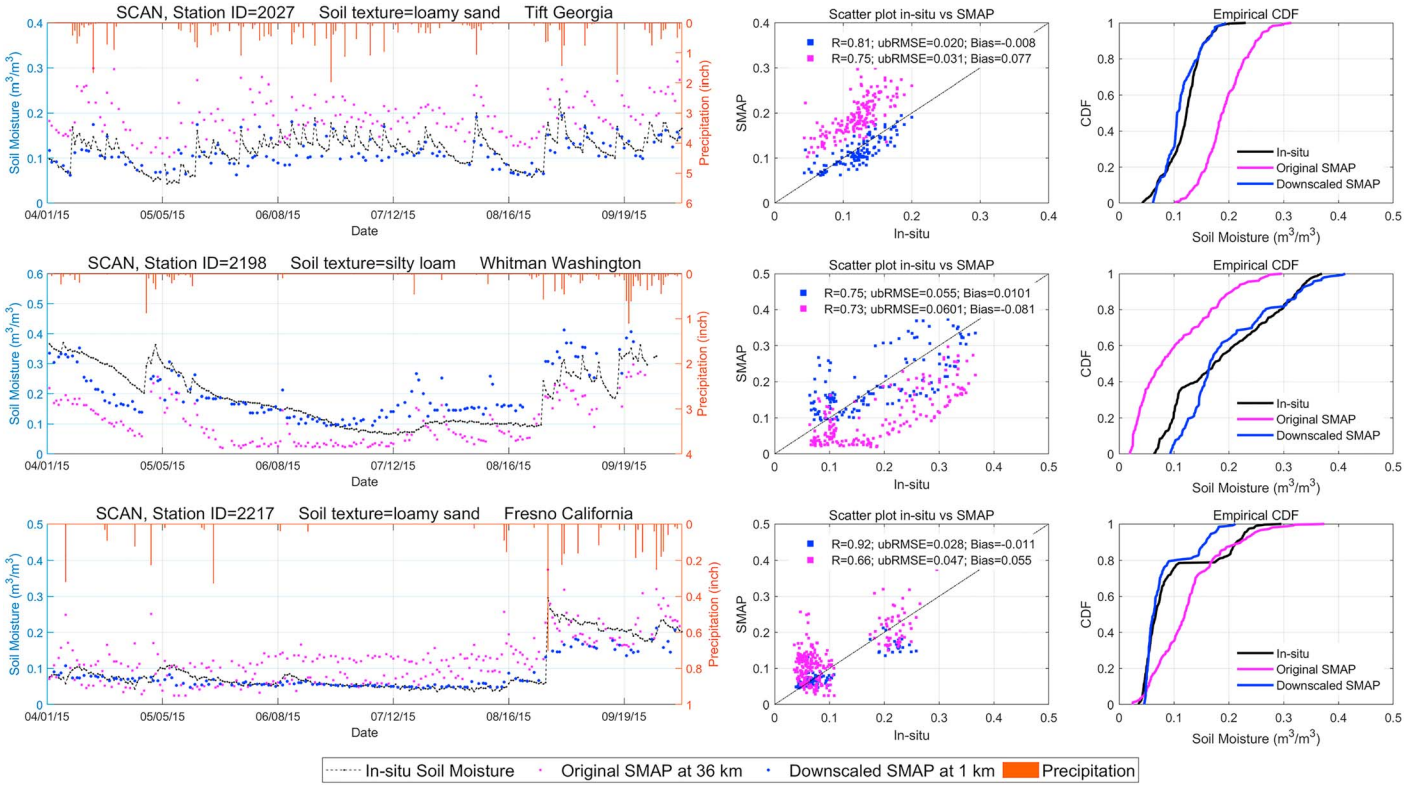

Figure 7. Time series, scatter plot, and CDF of original and downscaled SMAP soil moisture data versus in situ observations at top 5-cm depth. SCAN = Soil Climate Analysis Network; SMAP = Soil Moisture Active Passive; ubRMSE = unbiased Root Mean Square Error; CDF = Cumulative Distribution Function.

downscaled SMAP soil moisture by the proposed approach at three different SCAN in situ soil moisture stations located in different climate regimes. Figure S3 depicts these stations and their adjacent environment. The vegetation condition and climate regime of these three locations are summarized here to explain the downscaled soil moisture performance analysis. As mentioned earlier and is seen from Figure S3, although these in situ measurements do not represent the soil moisture heterogeneity within the SMAP footprint, they do represent the surrounding vegetation and land cover types. Station 2027 (Figure S3a) is instrumented in the Little River Experimental Watershed in Tift County, Georgia, where the prevailing climate is humid subtropical providing abundant rainfall throughout the year. The land use is a mixture of forest, crops, and pasture. Station 2198 (Figure S3b) is located in Whitman County, Washington. This region is mostly dominated by grassland and pasture and experiences a mild and temperate climate. October through April are the wettest months (often in the form of snow), while August is the driest month. Station 2217 (Figure S3c) is located in the semiarid Monocline Ridge area in Fresno County, California, where the climate is mostly characterized by hot and dry summers and mild and moist winters. In this area, the majority of precipitation falls during winter. Monocline Ridge is an uninhabited and unvegetated region.

Temporal variations of soil moisture from the downscaled SMAP (at 1 km), original SMAP (at 36 km), and in situ observations are illustrated along with precipitation (daily mean) in Figure 7, and their performance is evaluated using three statistical metrics, that is, *R*, ubRMSE (m^3/m^3), and bias (m^3/m^3). The detail information of each instrument including the station ID, soil texture type, and the location name are displayed in this figure. The black-dotted line and purple and blue points are indicating, respectively, the in situ soil moisture at 5 cm, the original SMAP soil moisture at top 5 cm, and the downscaled SMAP soil moisture time series. Although both SMAP products closely follow the precipitation patterns, their consistency against the in situ soil moisture observation differs based on the land-atmosphere characteristics. For example, in Tift County, Georgia, both original and downscaled SMAP data could well track the dynamics of the drying and wetting of soil moisture caused by precipitation. The original SMAP soil moisture noticed a significant amount of bias (Bias = 0.077 m^3/m^3) compared to the downscaled one (Bias = −0.008 m^3/m^3). This may be due to the

station's location where the dominant soil type is relatively well-drained loamy sand causing rapid soil drying after the precipitation event. The downscaled SMAP could capture this pattern properly, while the original SMAP failed to do so. The same analogy can be seen in Whitman County, Washington. In this station, the original SMAP underestimated the soil moisture almost throughout the whole period of study. This problem was mitigated by the downscaled SMAP soil moisture.

As mentioned above, although both SMAP products are reasonably able to reproduce the in situ soil moisture temporal dynamics, the original SMAP product may severely bias the soil moisture estimates. This issue was more clearly observed in the station 2217, which is located in Fresno County, California, where the original SMAP overestimated the soil moisture almost all days over the study period. This is mainly because fine- and coarser-resolution soil moisture observations often ignore the role of spatial scale differences in explaining differences between in situ and satellite soil moisture. In particular, the soil moisture dynamic range decreases by moving from small to large scale. The proposed downscaling algorithm is able to remove the systematic bias from the SMAP soil moisture when rescaling it to a finer resolution. For all three stations investigated here, the Cumulative Distribution Function in Figure 7 shows that the Cumulative Distribution Function of the downscaled SMAP perfectly matches with that of the in situ measurements. This further supports the effectiveness of the proposed algorithm in rescaling the coarse-resolution SMAP soil moisture, while reducing the mismatch between that and in situ observations. The statistical measures that are reported in this figure indicate that great improvement was made by the downscaled soil moisture data. It is worth mentioning that although the original SMAP soil moisture retrievals are validated using those stations that are not within the USCRN and SCAN soil moisture networks (at the time of study), they are in good agreement with these sparse in situ stations (Zhang et al., 2017). In Figure 7, the correlation coefficient and ubRMSE calculated between the original SMAP and in situ observations imply this link between the two.

4.2.2. Downscaled Soil Moisture Spatial Heterogeneity

Up to this point, we discussed how the downscaled soil moistures could capture the mean and amplitude of variations of in situ observations over different geographical locations with different land-atmosphere regimes. The ensuing task is to investigate the spatial consistency between the coarse- and fine-resolution soil moisture maps. The soil moisture spatial pattern is dependent on the heterogeneity of soil parameters (e.g., soil texture, vegetation, and topography) that are generally not distributed homogenously in the area. This results in an uncertainty in the soil moisture retrievals, which consequently affects the downscaled soil moisture accuracy (Piles et al., 2011). Here we try to assess the extent to which the downscaled soil moisture map could fill this gap and contribute to decreasing the discrepancy between the spatial variability of soil parameters and soil moistures. Figure 8 demonstrates an example of the original SMAP soil moisture data and the downscaled soil moisture on 27 April 2015, over the western CONUS. This figure also illustrates the land cover distribution. Figure 8 indicates that the spatial pattern of downscaled SMAP soil moisture (Figure 8c) closely follows the spatial heterogeneity of soil parameters such as vegetation cover (Figure 8a) and topography (previously shown in Figure S2). Likewise, the downscaled soil moisture data (Figure 8) closely matches the spatial pattern of the original soil moisture data (Figure 8b) across almost the entire western CONUS. Discrepancies between the original and downscaled data mostly occur in densely vegetated areas (i.e., evergreen and deciduous forests) where the SMAP soil moisture is prone to underestimation due to the attenuation of microwave signal by vegetation.

According to Figure 8, the downscaled SMAP soil moisture shows comparatively more water content in the topsoil layer than original SMAP. This is because the downscaled soil moisture at 1 km is obtained based on the soil moisture at point scale. Therefore, the fine-resolution SMAP product will lead to a lower soil moisture, similar to the one observed by SMAP satellite, if it is averaged to a coarser spatial scale. Another plausible reason behind this, is the fact that SMAP is measuring a large-scale average, and the averaging process dissipates anomalies more rapidly compared to the point (in situ) scale, leading to a faster drydown time scale (Shellito & Small, 2017; Shellito et al., 2016). Here the downscaled SMAP soil moistures are obtained using the model that is calibrated by in situ observations. It was found that the downscaled soil moistures are slightly wetter than the original SMAP product following rainfall events while correlating well with the in situ observations. Chen et al. (2017) showed that although SMAP retrievals underestimate soil moisture, they capture its dynamics well. Therefore, our conclusion is consistent with that of Chen et al. (2017). The downscaled SMAP soil moistures generated in this study are shown to track the dynamics of in situ observations well and

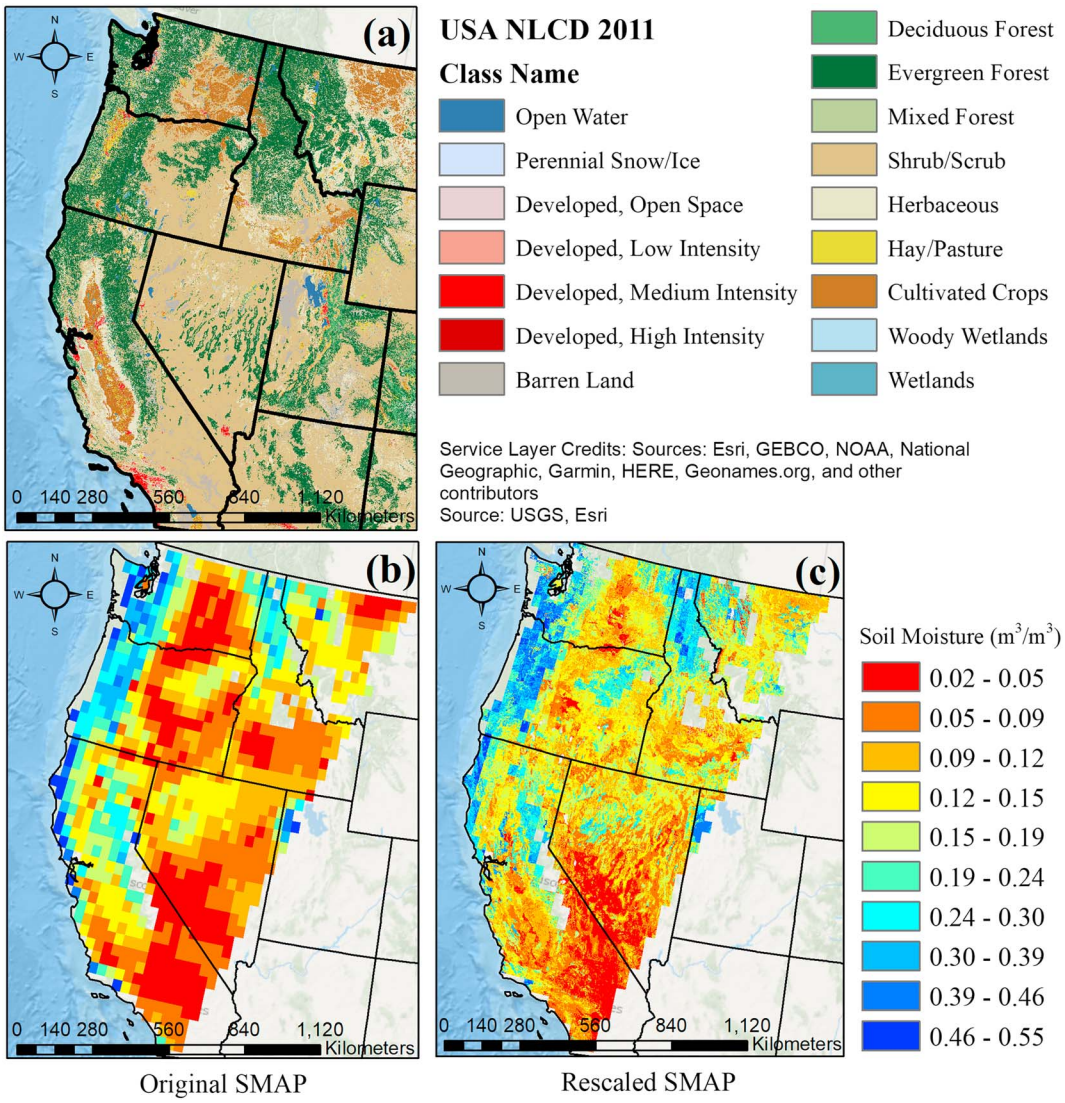

Figure 8. (a) Land cover distribution over the western Continental United States, (b) original SMAP soil moisture at 36-km spatial resolution, and (c) downscaled SMAP soil moisture at 1-km spatial resolution on 27 April 2015. SMAP = Soil Moisture Active Passive.

clearly capture the spatial heterogeneity of soil parameters with high spatial correspondence to the original SMAP soil moisture data.

The accuracy of downscaled soil moisture product in this study appears to be very good as compared to, for example, Mishra et al. (2018), who reported the CONUS average correlation between the thermal-infrared downscaled SMAP (passive) and SCAN is around 0.54, while in this study, the correlation between the downscaled SMAP product and SCAN networks is 0.65. However, it is noted that the successful use of a downscaling approach may be restricted to its certain characteristics and needs of a user, knowing that each method may have certain strengths and weaknesses (Chakrabarti et al., 2015, 2018; Chakrabarti, Judge, et al., 2016; Colliander, Fisher, et al., 2017). For example, in the work by Colliander, Fisher, et al. (2017), the authors proposed a disaggregation approach to downscale the SMAP soil moisture over a small domain (including three 36-km SMAP pixels), where the surface temperature is controlled by soil evaporation, the topographical variation is relatively moderate, and the vegetation density is relatively low.

4.3. Validation of Downscaled SMAP Soil Moisture Product

In these subsections, we evaluate the accuracy of downscaled SMAP soil moisture against two densely instrumented watersheds located in two different geographical zones in CONUS. In addition, in order to fully assess

Table 2
Comparison Between the Downscaled Soil Moisture Active Passive Soil Moisture at 1 km and In Situ Soil Moisture Measurements Within Little Washita River Watershed in 2015 (Location Information Is Based on the WGS84 Datum)

				Proposed downscaling approach			Uniform disaggregation approach		
Station ID	Soil texture	Latitude	Longitude	ubRMSE (m^3/m^3)	Bias (m^3/m^3)	*R*	ubRMSE (m^3/m^3)	Bias (m^3/m^3)	*R*
121	L	34.9586	−97.8986	—	—	—	—	—	—
124	SL	34.9728	−98.0581	0.036	0.008	0.802	0.048	0.016	0.759
131	SIL	34.9503	−98.2336	0.04	−0.004	0.872	0.036	−0.028	0.804
132	S	34.9428	−98.1819	0.034	0.027	0.861	0.051	0.114	0.588
133	S	34.9492	−98.1281	0.04	−0.02	0.741	0.042	0.08	0.719
136	L	34.9278	−97.9656	—	—	—	—	—	—
146	L	34.8853	−98.0231	0.048	−0.079	0.787	0.05	−0.025	0.604
148	SIL	34.8992	−98.1281	0.036	−0.001	0.825	0.047	−0.038	0.766
152	L	34.8611	−98.2511	0.039	−0.032	0.749	0.048	−0.008	0.719
154	L	34.8553	−98.1369	0.063	−0.032	0.874	0.046	−0.01	0.802
159	SL	34.7967	−97.9933	0.03	0.038	0.85	0.031	0.058	0.781
134	SL	34.92745	−98.075452	0.026	−0.012	0.913	0.044	0.039	0.773
135	L	34.93346	−98.018777	0.02	−0.015	0.847	0.046	0.113	0.763
144	L	34.86071	−97.91114	0.03	−0.051	0.841	0.043	−0.039	0.594
149	SIL	34.89139	−98.181246	0.038	−0.008	0.787	0.049	−0.042	0.872
150	SIL	34.90525	−98.25106	0.021	−0.005	0.773	0.046	0.01	0.866
153	L	34.85872	−98.199458	0.029	−0.069	0.815	0.057	−0.044	0.718
156	SL	34.83896	−97.962534	0.033	0.06	0.857	0.051	0.068	0.828
162	SL	34.79735	−98.126933	0.048	−0.011	0.857	0.035	−0.095	0.67
182	SL	34.84504	−98.073473	0.02	0.045	0.777	0.042	0.083	0.74
Average				0.035	−0.009	0.824	0.045	0.014	0.742

Note. ubRMSE = unbiased Root Mean Square Error.

the performance of the proposed downscaling algorithm, similar to section 4.2, the results are also compared with those obtained from the uniform disaggregation approach.

4.3.1. Study Area (1): Little Washita River Watershed

The Little Washita River Watershed is located in southwest Oklahoma in the Great Plains region of the United States and comprises an area of 610 km^2. A wide range of textures covers the watershed's surface layer, of which, sandy clay loam is the most dominant. There is a network of 20 in situ soil moisture stations distributed evenly over the entire watershed. This is called the Agricultural Research Service's Micronet. These stations are equipped with capacitance probes that record the soil moisture at a depth of approximately 3 to 7 cm with an hourly measurement interval. Many of these sensors also provide surface temperature measurements. In this study, the data set was collected daily for the period of 01 April 2015 to 31 December 2015 in order to be consistent with the period of available SMAP satellite data.

4.3.1.1. Validation Results Based on Little Washita River Watershed

The results reported in Table 2 indicate that the downscaled SMAP soil moisture product matches well with the in situ observations for the majority of stations, except for a few stations (121 and 136) that are located along the mainstream of the watershed at low altitudes, hence more prone to accumulation of soil moisture storage. Despite this concern, the majority of stations located within the watershed are showing satisfactory results (Table 2) which further validate the effectiveness of the RF approach. For the proposed downscaling method, the average values of ubRMSE, bias, and *R* across all stations are reported 0.035 m^3/m^3, −0.009 m^3/m^3, and 0.824, respectively, which are better than those from the uniform disaggregation approach. As seen in Table 2, the ubRMSE value for all soil types are less than the SMAP mission accuracy target of 0.04 m^3/m^3 (Jackson et al., 2016). However, for the uniform disaggregation approach, this value slightly exceeds the SMAP accuracy requirement.

The results affirm that the downscaled SMAP soil moisture not only captures the spatial distribution of soil moisture (as shown in Table 2) but also adequately monitors its temporal dynamics. The time series of downscaled SMAP soil moistures versus in situ observations at 20 Micronet stations were examined. The results showed that the downscaled soil moistures across all 20 stations closely follow the dynamics of in

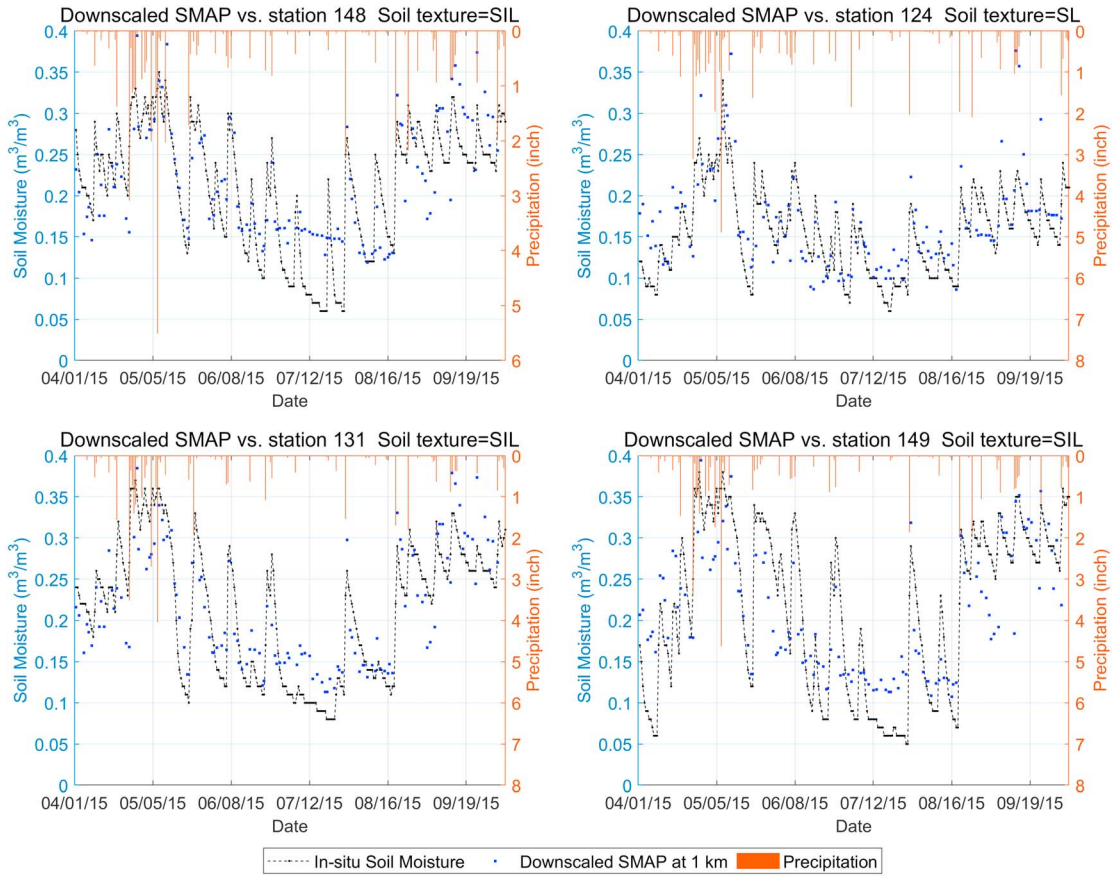

Figure 9. Daily in situ and downscaled SMAP radiometer soil moisture at 1 km along with precipitation observation for stations 148, 124, 131, and 149. SMAP = Soil Moisture Active Passive.

situ observations and precipitation pattern, such as dry-down and wet-up periods. For example, Figure 9 illustrates time-series comparisons between the downscaled SMAP soil moistures and in situ observations from a few selected stations (i.e., station 148, 124, 131, and 149) between 01 April 2015 and 31 December 2015.

4.3.2. Study Area (2): WGEW

The Walnut Gulch Experimental Watershed (WGEW) is one of two Agricultural Research Service experimental watersheds on western rangelands located in the southeastern Arizona with an area of 149 km^2. The predominant soil surface over this watershed is loamy. There are 19 soil moisture stations (identified as RG##) uniformly situated inside the watershed monitoring soil moisture every 30 min at a depth of approximately 3 to 7 cm. These sensors also measure soil temperature and precipitation. In this paper, the data sets are collected daily (hourly averaged) from 01 April 2015 to 31 December 2015, so as to be consistent with the time period of the current study.

4.3.2.1. Validation Results Based on WGEW

The results reported in Table 3 imply a satisfactory performance of the downscaled SMAP soil moisture product versus in situ observations for the majority of stations, except for a couple of stations (e.g., stations RG076 and RG092) situated close to the outlet of the watershed. The reason behind this may be attributed to the locations of these stations which were determined to accommodate the hydrologic research objectives of the watershed, not to validate the satellite soil moisture data products (Colliander, Cosh, et al., 2017). In the proposed downscaling method, the average values of ubRMSE, bias, and R across all stations (0.029 m^3/m^3, 0.008 m^3/m^3, and 0.637) are found to be more accurate than those from the uniform disaggregation approach (0.039 m^3/m^3, −0.002 m^3/m^3, and 0.517). More importantly, on average, the ubRMSE value for this watershed (0.029 m^3/m^3) is much lower than the SMAP mission accuracy target of 0.04 m^3/m^3. This indicates a successful application of the proposed algorithm for downscaling satellite soil moisture data.

Table 3
Comparison Between the Downscaled Soil Moisture Active Passive Soil Moisture at 1 km and In Situ Soil Moisture Measurements Within Walnut Gulch Experimental Watershed in 2015 (Location Information is Based on the WGS84 Datum)

Station ID	Soil texture	Latitude	Longitude	Proposed downscaling approach			Uniform disaggregation approach		
				ubRMSE (m^3/m^3)	Bias (m^3/m^3)	*R*	ubRMSE (m^3/m^3)	Bias (m^3/m^3)	*R*
RG003	L	31.72044	−110.14294	0.039	0.001	0.58	0.051	0.016	0.207
RG013	L	31.7238	−110.0911	0.031	−0.002	0.644	0.043	−0.057	0.472
RG014	L	31.69683	−110.09869	0.026	−0.041	0.691	0.033	0.011	0.594
RG018	L	31.70487	−110.08492	0.032	−0.037	0.435	0.039	0.007	0.39
RG020	L	31.6761	−110.07712	0.025	0.027	0.729	0.037	−0.002	0.471
RG028	L	31.72201	−110.0434	0.03	0.013	0.637	0.029	−0.005	0.709
RG034	L	31.69886	−110.0403	0.031	0.042	0.477	0.033	0.012	0.603
RG037	L	31.68613	−110.01556	0.028	0.064	0.448	0.045	0.054	0.149
RG040	L	31.72429	−110.01431	0.023	0.019	0.783	0.03	−0.006	0.662
RG046	L	31.70931	−109.99436	0.065	0.011	0.677	0.057	−0.03	0.634
RG057	L	31.72842	−109.98571	0.028	0.001	0.853	0.032	−0.026	0.681
RG069	L	31.76997	−109.9026	0.021	0.005	0.607	0.053	−0.062	0.706
RG070	L	31.75861	−109.89881	0.024	0.084	0.583	0.027	0.023	0.75
RG076	L	31.71956	−110.12815	—	—	—	—	—	—
RG082	L	31.73618	−109.94271	0.032	−0.014	0.631	0.037	−0.032	0.586
RG083	L	31.74377	−110.05292	0.015	−0.058	0.719	0.031	0.045	0.671
RG089	L	31.75682	−109.98308	0.02	−0.032	0.673	0.06	−0.028	−0.126
RG092	L	31.7386	−110.13545	—	—	—	—	—	—
RG100	L	31.67398	−110.01608	0.026	0.06	0.641	0.031	0.03	0.645
Average				0.029	0.008	0.637	0.039	−0.002	0.517

Note. unbiased Root Mean Square Error.

We examined the temporal variation of downscaled soil moisture data set and found that they are able to capture the dynamics of in situ observations well. Further investigation also revealed that discrepancies between downscaled and in-situ soil moistures mostly occur during the North American Monsoon season when the spatial distribution of soil moisture over WGEW is more heterogeneous.

Using two CVSs, we summarize the accuracy of both downscaling approaches in Figure 10. It is observed that the proposed downscaling approach outperforms the uniform disaggregation approach for all performance measures used. It is also noted that when the downscaled SMAP soil moisture (or the original SMAP) is compared with in situ observation for validation purposes, an unavoidable significant discrepancy between these two sets of data exacerbates the analysis. This is due to inherent properties of each observation. SMAP

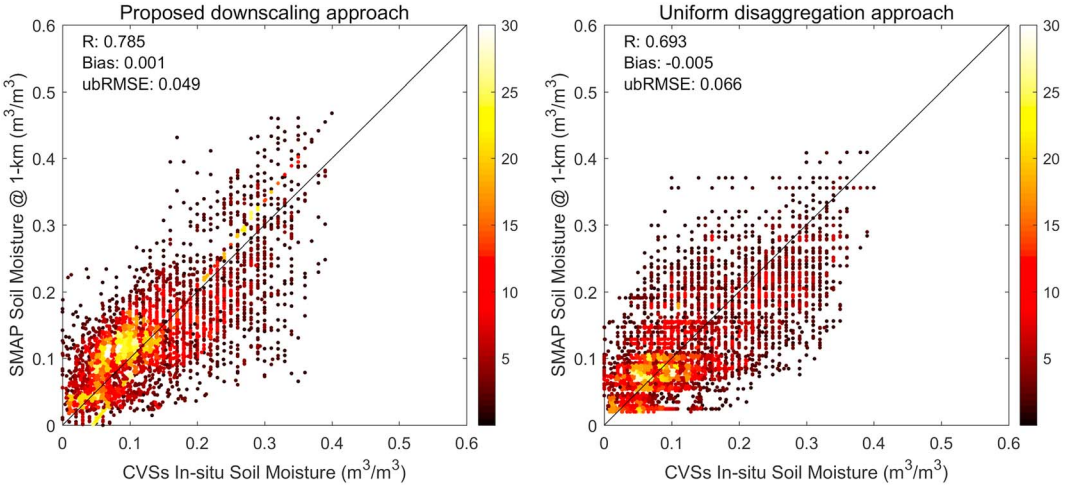

Figure 10. Comparison between the soil moisture retrieved from CVSs and those downscaled by two downscaling approaches used in this study. SMAP = Soil Moisture Active Passive; ubRMSE = unbiased Root Mean Square Error; CVS = Core Validation Site.

measures a large-scale average of soil moisture, while in situ station measures soil moisture at specific point. Even if all CVS in situ observations within the downscaled or original SMAP grid cells are averaged to represent the soil moisture, significant differences are still to be expected.

5. Summary and Conclusion

This paper presents a new framework based on an ensemble learning algorithm to downscale SMAP radiometer soil moisture from its native resolution of 36 km to a finer resolution of 1 km while using atmospheric and geophysical information acquired from high-resolution remote-sensing data and ground-based observations. The data sets used in the proposed model have been widely utilized in many studies for rescaling satellite soil moisture data and are similar to those ancillary data used in SMAP level 2 Enhanced Passive Soil Moisture Product (L2_SM_P_E) and standard L2_SM_P (Chan et al., 2017). This study was performed for the period of 9 months (01 April 2015 to 31 December 2015) over the CONUS. The validation results based on in situ soil moisture measurements collected from two CVSs and 300 sparse soil moisture networks confirmed that the downscaled SMAP soil moistures would adequately meet the SMAP soil moisture retrieval accuracy requirement (ubRMSE = 0.040 m^3/m^3) and capture the spatial heterogeneity of soil parameters and dynamics of in situ soil moisture observations. The downscaled soil moisture data obtained from the proposed downscaling approach is also compared with those from the uniform disaggregation approach over both CVSs and 300 soil moisture networks, and in all cases, the proposed approach outperformed the uniform disaggregation approach. The results of this study also revealed that the inclusion of all input variables would result in best downscaling accuracy; however, the topography data were found to affect the results less than other input variables. The other merit of the proposed methodology is that it is not restricted to boundary conditions such as semiarid or humid regions, and it can be applied over a large area with different climatological patterns and soil characteristics.

The proposed rescaling model was calibrated using 300 sparse in situ soil moisture sensors evenly distributed over the CONUS. Future works may consider using other in situ observations from different operational networks, such as COSMOS (Zreda et al., 2012) and GPS (Larson et al., 2010), and some others available from the International Soil Moisture Network (Kim et al., 2017) for model calibration and validation purposes.

Acknowledgments
Partial financial support for this project was provided through NOAA grant NA18OAR4310319. We appreciate all who have provided high-quality in situ soil moisture data for Little Washita River Watershed (http://ars.mesonet.org/), Walnut Gulch Experimental Watershed (https://www.tucson.ars.ag.gov/dap/), USCRN (https://www.ncdc.noaa.gov/crn/usrcrn/), and SCAN (https://www.wcc.nrcs.usda.gov/scan/) soil moisture networks. We also greatly thank two anonymous reviewers for constructive comments that improved the earlier version of this article.

References

Alemohammad, S. H., Kolassa, J., Prigent, C., Aires, F., & Gentine, P. (2018). Global downscaling of remotely-sensed soil moisture using neural networks. *Hydrology and Earth System Sciences Discussions*, 1–19. https://doi.org/10.5194/hess-2017-680

Amit, Y., & Geman, D. (1997). Shape quantization and recognition with randomized trees. *Neural Computation*, *9*(7), 1545–1588. https://doi.org/10.1162/neco.1997.9.7.1545

Breiman, L. (2001). Random forests. *Machine Learning*, *45*(1), 5–32. https://doi.org/10.1023/A:1010933404324

Busch, F. A., Niemann, J. D., & Coleman, M. (2012). Evaluation of an empirical orthogonal function-based method to downscale soil moisture patterns based on topographical attributes. *Hydrological Processes*, *26*(18), 2696–2709. https://doi.org/10.1002/hyp.8363

Chakrabarti, S., Bongiovanni, T., Judge, J., Nagarajan, K., & Principe, J. C. (2015). Downscaling satellite-based soil moisture in heterogeneous regions using high-resolution remote sensing products and information theory: A synthetic study. *IEEE Transactions on Geoscience and Remote Sensing*, *53*(1), 85–101. https://doi.org/10.1109/TGRS.2014.2318699

Chakrabarti, S., Bongiovanni, T., Judge, J., Rangarajan, A., & Ranka, S. (2016). Disaggregation of SMAP L3 brightness temperatures to 9km using kernel machines. *IEEE Geoscience and Remote Sensing Letters*. arXiv:1601.05350v2

Chakrabarti, S., Judge, J., Bongiovanni, T., Rangarajan, A., & Ranka, S. (2016). Disaggregation of remotely sensed soil moisture in heterogeneous landscapes using holistic structure-based models. *IEEE Transactions on Geoscience and Remote Sensing*, *54*(8), 4629–4641. https://doi.org/10.1109/TGRS.2016.2547389

Chakrabarti, S., Judge, J., Bongiovanni, T., Rangarajan, A., & Ranka, S. (2018). Spatial scaling using temporal correlations and ensemble learning to obtain high-resolution soil moisture. *IEEE Transactions on Geoscience and Remote Sensing*, *56*(3), 1238–1250. https://doi.org/10.1109/TGRS.2017.2722236

Chan, S. K., Bindlish, R., O'Neill, P., Jackson, T., Njoku, E., Dunbar, S., et al. (2017). Development and assessment of the SMAP enhanced passive soil moisture product. *Remote Sensing of Environment*, *204*, 931–941. https://doi.org/10.1016/j.rse.2017.08.025

Chan, S. K., Bindlish, R., O'Neill, P. E., Njoku, E., Jackson, T., Colliander, A., et al. (2016). Assessment of the SMAP passive soil moisture product. *IEEE Transactions on Geoscience and Remote Sensing*, *54*(8), 4994–5007. https://doi.org/10.1109/TGRS.2016.2561938

Chen, Y., Yang, K., Qin, J., Cui, Q., Lu, H., La, Z., et al. (2017). Evaluation of SMAP, SMOS, and AMSR2 soil moisture retrievals against observations from two networks on the Tibetan Plateau. *Journal of Geophysical Research: Atmospheres*, *122*, 5780–5792. https://doi.org/10.1002/2016JD026388

Choi, M., & Hur, Y. (2012). A microwave-optical/infrared disaggregation for improving spatial representation of soil moisture using AMSR-E and MODIS products. *Remote Sensing of Environment*, *124*, 259–269. https://doi.org/10.1016/j.rse.2012.05.009

Coleman, M. L., & Niemann, J. D. (2013). Controls on topographic dependence and temporal instability in catchment-scale soil moisture patterns. *Water Resources Research*, *49*, 1625–1642. https://doi.org/10.1002/wrcr.20159

Colliander, A., Cosh, M. H., Misra, S., Jackson, T. J., Crow, W. T., Chan, S., et al. (2017). Validation and scaling of soil moisture in a semi-arid environment: SMAP validation experiment 2015 (SMAPVEX15). *Remote Sensing of Environment*, *196*, 101–112. https://doi.org/10.1016/j.rse.2017.04.022

Colliander, A., Fisher, J. B., Halverson, G., Merlin, O., Misra, S., Bindlish, R., et al. (2017). Spatial downscaling of SMAP soil moisture using MODIS land surface temperature and NDVI during SMAPVEX15. *IEEE Geoscience and Remote Sensing Letters*, *14*(11), 2107–2111. https://doi.org/10.1109/LGRS.2017.2753203

Colliander, A., Jackson, T. J., Bindlish, R., Chan, S., Das, N., Kim, S. B., et al. (2017). Validation of SMAP surface soil moisture products with core validation sites. *Remote Sensing of Environment*, *191*, 215–231. https://doi.org/10.1016/j.rse.2017.01.021

Coopersmith, E. J., Bell, J. E., & Cosh, M. H. (2015). Extending the soil moisture data record of the U.S. climate reference network (USCRN) and soil climate analysis network (SCAN). *Advances in Water Resources*, *79*, 80–90. https://doi.org/10.1016/j.advwatres.2015.02.006

Coulibaly, P., Dibike, Y. B., & Anctil, F. (2005). Downscaling precipitation and temperature with temporal neural networks. *Journal of Hydrometeorology*, *6*(4), 483–496. https://doi.org/10.1175/JHM409.1

Crow, W. T., Berg, A. A., Cosh, M. H., Loew, A., Mohanty, B. P., Panciera, R., et al. (2012). Upscaling sparse ground-based soil moisture observations for the validation of coarse-resolution satellite soil moisture products. *Reviews of Geophysics*, *50*, RG2002. https://doi.org/10.1029/2011RG000372

Djamai, N., Magagi, R., Goïta, K., Merlin, O., Kerr, Y., & Roy, A. (2016). A combination of DISPATCH downscaling algorithm with CLASS land surface scheme for soil moisture estimation at fine scale during cloudy days. *Remote Sensing of Environment*, *184*, 1–14. https://doi.org/10.1016/j.rse.2016.06.010

Djamai, N., Magagi, R., Goita, K., Merlin, O., Kerr, Y., & Walker, A. (2015). Disaggregation of SMOS soil moisture over the Canadian prairies. *Remote Sensing of Environment*, *170*, 255–268. https://doi.org/10.1016/j.rse.2015.09.013

Entekhabi, B. D., Njoku, E. G., Neill, P. E. O., Kellogg, K. H., Crow, W. T., Edelstein, W. N., et al. (2010). The Soil Moisture Active Passive (SMAP) Mission. *Proceedings of the IEEE*, *98*(5), 704–716. https://doi.org/10.1109/JPROC.2010.2043918

Entekhabi, D., Reichle, R. H., Koster, R. D., & Crow, W. T. (2010). Performance metrics for soil moisture retrievals and application requirements. *Journal of Hydrometeorology*, *11*(3), 832–840. https://doi.org/10.1175/2010JHM1223.1

Fang, B., & Lakshmi, V. (2014). Soil moisture at watershed scale: Remote sensing techniques. *Journal of Hydrology*, *516*, 258–272. https://doi.org/10.1016/j.jhydrol.2013.12.008

Gan, Y., Duan, Q., Gong, W., Tong, C., Sun, Y., Chu, W., et al. (2014). A comprehensive evaluation of various sensitivity analysis methods: A case study with a hydrological model. *Environmental Modelling and Software*, *51*, 269–285. https://doi.org/10.1016/j.envsoft.2013.09.031

Goyal, M. K., Burn, D. H., & Ojha, C. S. P. (2012). Evaluation of machine learning tools as a statistical downscaling tool: Temperatures projections for multi-stations for Thames River Basin, Canada. *Theoretical and Applied Climatology*, *108*(3–4), 519–534. https://doi.org/10.1007/s00704-011-0546-1

Hashmi, M. Z., Shamseldin, A. Y., & Melville, B. W. (2011). Statistical downscaling of watershed precipitation using Gene Expression Programming (GEP). *Environmental Modelling & Software*, *26*(12), 1639–1646. https://doi.org/10.1016/j.envsoft.2011.07.007

He, X., Chaney, N. W., Schleiss, M., & Sheffield, J. (2016). Spatial downscaling of precipitation using adaptable random forests. *Water Resources Research*, *52*, 8217–8237. https://doi.org/10.1002/2016WR019034

Hutengs, C., & Vohland, M. (2016). Downscaling land surface temperatures at regional scales with random forest regression. *Remote Sensing of Environment*, *178*, 127–141. https://doi.org/10.1016/j.rse.2016.03.006

Im, J., Park, S., Rhee, J., Baik, J., & Choi, M. (2016). Downscaling of AMSR-E soil moisture with MODIS products using machine learning approaches. *Environmental Earth Sciences*, *75*(15), 1–19. https://doi.org/10.1007/s12665-016-5917-6

Jackson, T., Colliander, A., Kimball, J., Reichle, R., Crow, W., Entekhabi, D., & Neill, P. O. (2012). Science data calibration and validation plan.

Jackson, T. J., O'Neill, P., Njoku, E., Chan, S., Bindlish, R., Colliander, A., et al. (2016). Soil Moisture Active Passive (SMAP) project calibration and validation for the L2/3_SM_P version 3 data products, (SMAP Project), JPL D-93720, Jet Propulsion Laboratory, Pasadena.

Jing, W., Yang, Y., Yue, X., & Zhao, X. (2016). A spatial downscaling algorithm for satellite-based precipitation over the Tibetan plateau based on NDVI, DEM, and land surface temperature. *Remote Sensing*, *8*(8), 655. https://doi.org/10.3390/rs8080655

Jones, A. R., & Brunsell, N. A. (2009). A scaling analysis of soil moisture-precipitation interactions in a regional climate model. *Theoretical and Applied Climatology*, *98*(3–4), 221–235. https://doi.org/10.1007/s00704-009-0109-x

Kaheil, Y. H., Gill, M. K., Mckee, M., Bastidas, L. A., & Rosero, E. (2008). Downscaling and assimilation of surface soil moisture using ground truth measurements. *IEEE Transactions on Geoscience and Remote Sensing*, *46*(5), 1375–1384.

Ke, Y., Im, J., Park, S., & Gong, H. (2016). Downscaling of MODIS one kilometer evapotranspiration using Landsat-8 data and machine learning approaches. *Remote Sensing*, *8*(3), 1–26. https://doi.org/10.3390/rs8030215

Kerr, Y. H. (2007). Soil moisture from space: Where are we? *Hydrogeology Journal*, *15*(1), 117–120. https://doi.org/10.1007/s10040-006-0095-3

Kim, G., & Barros, A. P. (2002). Downscaling of remotely sensed soil moisture with a modified fractal interpolation method using contraction mapping and ancillary data. *Remote Sensing of Environment*, *83*(3), 400–413. https://doi.org/10.1016/S0034-4257(02)00044-5

Kim, H., Parinussa, R., Konings, A. G., Wagner, W., Cosh, M. H., Lakshmi, V., et al. (2017). Global-scale assessment and combination of SMAP with ASCAT (active) and AMSR2 (passive) soil moisture products. *Remote Sensing of Environment*, 260–275. https://doi.org/10.1016/j.rse.2017.10.026

Kolassa, J., Reichle, R. H., Liu, Q., Alemohammad, S. H., Gentine, P., Aida, K., et al. (2018). Estimating surface soil moisture from SMAP observations using a neural network technique. *Remote Sensing of Environment*, *204*, 43–59. https://doi.org/10.1016/j.rse.2017.10.045

Larson, K. M., Braun, J. J., Small, E. E., Zavorotny, V. U., Gutmann, E. D., & Bilich, A. L. (2010). GPS multipath and its relation to near-surface soil moisture content. *IEEE Journal of Selected Topics in Applied Earth Observations and Remote Sensing*, *3*(1), 91–99. https://doi.org/10.1109/JSTARS.2009.2033612

Lievens, H., De Lannoy, G. J. M., Al Bitar, A., Drusch, M., Dumedah, G., Hendricks Franssen, H. J., et al. (2016). Assimilation of SMOS soil moisture and brightness temperature products into a land surface model. *Remote Sensing of Environment*, *180*, 292–304. https://doi.org/10.1016/j.rse.2015.10.033

Ma, C., Li, X., Wei, L., & Wang, W. (2017). Multi-scale validation of SMAP soil moisture products over cold and arid regions in Northwestern China using distributed ground observation data. *Remote Sensing*, *9*(4). https://doi.org/10.3390/rs9040327

Mascaro, G., Vivoni, E. R., & Deidda, R. (2011). Soil moisture downscaling across climate regions and its emergent properties. *Journal of Geophysical Research*, *116*, D22114. https://doi.org/10.1029/2011JD016231

Mattikalli, N. M., Engman, E. T., Jackson, T. J., & Ahuja, L. R. (1998). Microwave remote sensing of temporal variations of brightness temperature and near-surface soil water content during a watershed-scale field experiment, and its application to the estimation of soil physical properties. *Water Resources Research*, *34*(9), 2289–2299. https://doi.org/10.1029/98WR00553

Merlin, O., Malbéteau, Y., Notfi, Y., Bacon, S., Er-Raki, S., Khabba, S., & Jarlan, L. (2015). Performance metrics for soil moisture downscaling methods: Application to DISPATCH data in central Morocco. *Remote Sensing*, *7*(4), 3783–3807. https://doi.org/10.3390/rs70403783

Merlin, O., Walker, J. P., Chehbouni, A., & Kerr, Y. (2008). Towards deterministic downscaling of SMOS soil moisture using MODIS derived soil evaporative efficiency. *Remote Sensing of Environment*, *112*(10), 3935–3946. https://doi.org/10.1016/j.rse.2008.06.012

Miller, D. A., & White, R. A. (1998). A conterminous United States multilayer soil characteristics dataset for regional climate and hydrology modeling. *Earth Interactions*, *2*(2), 1–26.
Mishra, A., Vu, T., Veettil, A. V., & Entekhabi, D. (2017). Drought monitoring with soil moisture active passive (SMAP) measurements. *Journal of Hydrology*, *552*, 620–632. https://doi.org/10.1016/j.jhydrol.2017.07.033
Mishra, V., Ellenburg, W. L., Griffin, R. E., Mecikalski, J. R., Cruise, J. F., Hain, C. R., & Anderson, M. C. (2018). An initial assessment of a SMAP soil moisture disaggregation scheme using TIR surface evaporation data over the continental United States. *International Journal of Applied Earth Observation and Geoinformation*, *68*, 92–104. https://doi.org/10.1016/j.jag.2018.02.005
Molero, B., Merlin, O., Malbéteau, Y., Al Bitar, A., Cabot, F., Stefan, V., et al. (2016). SMOS disaggregated soil moisture product at 1 km resolution: Processor overview and first validation results. *Remote Sensing of Environment*, *180*, 361–376. https://doi.org/10.1016/j.rse.2016.02.045
Njoku, E. G., & Entekhabi, D. (1996). Passive microwave remote sensing of soil moisture. *Journal of Hydrology*, *184*(1–2), 101–129. https://doi.org/10.1016/0022-1694(95)02970-2
Owe, M., de Jeu, R., & Holmes, T. (2008). Multisensor historical climatology of satellite-derived global land surface moisture. *Journal of Geophysical Research*, *113*, F01002. https://doi.org/10.1029/2007JF000769
Pan, M., Cai, X., Chaney, N., Entekhabi, D., & Wood, E. F. (2016). An initial assessment of SMAP soil moisture retrievals using high resolution model simulations and in-situ observations. *Geophysical Research Letters*, *43*, 9662–9668. https://doi.org/10.1002/2016GL069964
Panciera, R., Walker, J. P., Kalma, J. D., Kim, E. J., Member, S., Hacker, J. M., et al. (2008). The NAFE 05 / CoSMOS data set : Toward SMOS soil moisture retrieval , downscaling , and assimilation. *Cosmos*, *46*(3), 736–745. https://doi.org/10.1109/TGRS.2007.915403
Park, S., Park, S., Im, J., Rhee, J., Shin, J., & Park, J. (2017). Downscaling GLDAS soil moisture data in East Asia through fusion of multi-sensors by optimizing modified regression trees. *Water*, *9*(5), 332. https://doi.org/10.3390/w9050332
Pellenq, J., Kalma, J., Boulet, G., Saulnier, G. M., Wooldridge, S., Kerr, Y., & Chehbouni, A. (2003). A disaggregation scheme for soil moisture based on topography and soil depth. *Journal of Hydrology*, *276*(1–4), 112–127. https://doi.org/10.1016/S0022-1694(03)00066-0
Pelletier, C., Valero, S., Inglada, J., Champion, N., & Dedieu, G. (2016). Assessing the robustness of random forests to map land cover with high resolution satellite image time series over large areas. *Remote Sensing of Environment*, *187*, 156–168. https://doi.org/10.1016/j.rse.2016.10.010
Peng, J., Loew, A., Zhang, S., & Wang, J. (2016). Spatial downscaling of global satellite soil moisture data using temperature vegetation dryness index. *IEEE Transactions on Geoscience and Remote Sensing*, *1*(54), 558–566.
Peng, J., Niesel, J., & Loew, A. (2015). Evaluation of soil moisture downscaling using a simple thermal-based proxy-the REMEDHUS network (Spain) example. *Hydrology and Earth System Sciences*, *19*(12), 4765–4782. https://doi.org/10.5194/hess-19-4765-2015
Petropoulos, G. P., Ireland, G., & Barrett, B. (2015). Surface soil moisture retrievals from remote sensing: Current status, products & future trends. *Physics and Chemistry of the Earth*, *83–84*, 36–56. https://doi.org/10.1016/j.pce.2015.02.009
Piles, M., Camps, A., Vall-Llossera, M., Corbella, I., Panciera, R., Rudiger, C., et al. (2011). Downscaling SMOS-derived soil moisture using MODIS visible/infrared data. *IEEE Transactions on Geoscience and Remote Sensing*, *49*(9), 3156–3166. https://doi.org/10.1109/TGRS.2011.2120615
Piles, M., Petropoulos, G. P., Sanchez, N., Gonzalez-Zamora, A., & Ireland, G. (2016). Towards improved spatio-temporal resolution soil moisture retrievals from the synergy of SMOS and MSG SEVIRI spaceborne observations. *Remote Sensing of Environment*, *180*, 403–417. https://doi.org/10.1016/j.rse.2016.02.048
Piles, M., Sánchez, N., Vall-Llossera, M., Camps, A., Martínez-Fernandez, J., Martinez, J., & Gonzalez-Gambau, V. (2014). A downscaling approach for SMOS land observations: Evaluation of high-resolution soil moisture maps over the Iberian peninsula. *IEEE Journal of Selected Topics in Applied Earth Observations and Remote Sensing*, *7*(9), 3845–3857. https://doi.org/10.1109/JSTARS.2014.2325398
Raje, D., & Mujumdar, P. P. (2011). A comparison of three methods for downscaling daily precipitation in the Punjab region. *Hydrological Processes*, *25*(23), 3575–3589. https://doi.org/10.1002/hyp.8083
Ranney, K. J., Niemann, J. D., Lehman, B. M., Green, T. R., & Jones, A. S. (2015). A method to downscale soil moisture to fine resolutions using topographic, vegetation, and soil data. *Advances in Water Resources*, *76*, 81–96. https://doi.org/10.1016/j.advwatres.2014.12.003
Reichle, R. H., Entekhabi, D., & McLaughlin, D. B. (2001). Downscaling of radio brightness measurements for soil moisture estimation: A four-dimensional variational data assimilation approach. *Water Resources Research*, *37*(9), 2353–2364. https://doi.org/10.1029/2001WR000475
Rodriguez-Fernandez, N. J., Aires, F., Richaume, P., Kerr, Y. H., Prigent, C., Kolassa, J., et al. (2015). Soil moisture retrieval using neural networks: Application to SMOS. *IEEE Transactions on Geoscience and Remote Sensing*, *53*(11), 5991–6007. https://doi.org/10.1109/TGRS.2015.2430845
Sahoo, A. K., De Lannoy, G. J. M., Reichle, R. H., & Houser, P. R. (2013). Assimilation and downscaling of satellite observed soil moisture over the Little River Experimental Watershed in Georgia, USA. *Advances in Water Resources*, *52*, 19–33. https://doi.org/10.1016/j.advwatres.2012.08.007
Sanchez, N., Piles, M., Scaini, A., Martinez-Fernandez, J., Camps, A., & Vall-Llossera, M. (2012). Spatial patterns of SMOS downscaled soil moisture maps over the remedhus network (Spain). *International Geoscience and Remote Sensing Symposium (IGARSS)*, 714–717. https://doi.org/10.1109/IGARSS.2012.6351465
Seneviratne, S. I., Corti, T., Davin, E. L., Hirschi, M., Jaeger, E. B., Lehner, I., et al. (2010). Investigating soil moisture-climate interactions in a changing climate: A review. *Earth-Science Reviews*, *99*(3–4), 125–161. https://doi.org/10.1016/j.earscirev.2010.02.004
Shellito, P. J., & Small, E. E. (2017). Controls on surface soil drying rates observed by SMAP and simulated by the Noah land surface model. *Hydrology and Earth System Sciences Discussions*, *22*, 1649–1663. https://doi.org/10.5194/hess-2017-338
Shellito, P. J., Small, E. E., Colliander, A., Bindlish, R., Cosh, M. H., Berg, A. A., et al. (2016). SMAP soil moisture drying more rapid than observed in situ following rainfall events. *Geophysical Research Letters*, *43*, 8068–8075. https://doi.org/10.1002/2016GL069946
Shin, Y., & Mohanty, B. P. (2013). Development of a deterministic downscaling algorithm for remote sensing soil moisture footprint using soil and vegetation classifications. *Water Resources Research*, *49*, 6208–6228. https://doi.org/10.1002/wrcr.20495
Song, C., Jia, L., & Menenti, M. (2014). Retrieving high-resolution surface soil moisture by downscaling AMSR-E brightness temperature using MODIS LST and NDVI data. *IEEE Journal of Selected Topics in Applied Earth Observations and Remote Sensing*, *7*(3), 935–942. https://doi.org/10.1109/JSTARS.2013.2272053
Srivastava, P. K., Han, D., Ramirez, M. R., & Islam, T. (2013). Machine learning techniques for downscaling SMOS satellite soil moisture using MODIS land surface temperature for hydrological application. *Water Resources Management*, *27*, 3127–3144. https://doi.org/10.1007/s11269-013-0337-9
Su, C. H., Ryu, D., Young, R. I., Western, A. W., & Wagner, W. (2013). Inter-comparison of microwave satellite soil moisture retrievals over the Murrumbidgee Basin, southeast Australia. *Remote Sensing of Environment*, *134*(2013), 1–11. https://doi.org/10.1016/j.rse.2013.02.016
Taylor, K. E. (2001). Summarizing multiple aspects of model performance in a single diagram. *Journal of Geophysical Research*, *106*(D7), 7183–7192. https://doi.org/10.1029/2000JD900719

Valverde, M. C., Araujo, E., & Campos Velho, H. (2014). Neural network and fuzzy logic statistical downscaling of atmospheric circulation-type specific weather pattern for rainfall forecasting. *Applied Soft Computing Journal*, *22*, 681–694. https://doi.org/10.1016/j.asoc.2014.02.025

Velpuri, N. M., Senay, G. B., & Morisette, J. T. (2015). Evaluating new SMAP soil moisture for drought monitoring in the rangelands of the US High Plains. *Rangelands*, *38*(4), 183–190. https://doi.org/10.1016/j.rala.2016.06.002

Verhoest, N. E. C., Lievens, H., Wagner, W., Alvarez-Mozos, J., Moran, M. S., & Mattia, F. (2008). On the soil roughness parameterization problem in soil moisture retrieval of bare surfaces from synthetic aperture radar. *Sensors*, *8*(7), 4213–4248. https://doi.org/10.3390/s8074213

Wagner, W., Hahn, S., Kidd, R., Melzer, T., Bartalis, Z., Hasenauer, S., et al. (2013). The ASCAT soil moisture product: A review of its specifications, validation results, and emerging applications. *Meteorologische Zeitschrift*, *22*(1), 5–33. https://doi.org/10.1127/0941-2948/2013/0399

Wilson, D. J., Western, A. W., & Grayson, R. B. (2005). A terrain and data-based method for generating the spatial distribution of soil moisture. *Advances in Water Resources*, *28*(1), 43–54. https://doi.org/10.1016/j.advwatres.2004.09.007

Zerenner, T., Venema, V., Friederichs, P., & Simmer, C. (2016). Downscaling near-surface atmospheric fields with multi-objective genetic programming. *Environmental Modelling and Software*, *84*, 85–98. https://doi.org/10.1016/j.envsoft.2016.06.009

Zhang, X., Zhang, T., Zhou, P., Shao, Y., & Gao, S. (2017). Validation analysis of SMAP and AMSR2 soil moisture products over the United States using ground-based measurements. *Remote Sensing*, *9*(2). https://doi.org/10.3390/rs9020104

Zhao, W., & Li, A. (2013). A downscaling method for improving the spatial resolution of AMSR-E derived soil moisture product based on MSG-SEVIRI data. *Remote Sensing*, *5*(12), 6790–6811. https://doi.org/10.3390/rs5126790

Zreda, M., Shuttleworth, W. J., Zeng, X., Zweck, C., Desilets, D., Franz, T., & Rosolem, R. (2012). COSMOS: The cosmic-ray soil moisture observing system. *Hydrology and Earth System Sciences*, *16*(11), 4079–4099. https://doi.org/10.5194/hess-16-4079-2012